Natural Product Chemical Study on Biologically Acitive Secondary Metabolites Produced by Phytopathogenic Fungi

植物病原菌が生産する生理活性二次代謝産物に関する天然物化学的研究

Masanobu Suzuki

鈴木　大進

2013

Contents

LIST OF ABBREVIATIONS USED

AcOH	acetic acid
BSA	bovine serum albumin
CC	column chromatography
CD	circular dichroism
CI-MS	chemical ionization mass spectrometry
DMF	dimethyl formamide
DMSO	dimethyl sulfoxide
DNA	deoxyribonucleic acid
EDTA	2-({2-[bis(carboxymethyl)amino]ethyl}(carboxymethyl)amino) acetic acid.
EI-MS	electron ionization mass spectrometry
EtOAc	ethyl acetate
ESI-TOFMS	electrospray ionization time-of-flight mass spectrometry
EtOH	ethanol
FAD	flavin adenine dinucleotide
^{1}H-^{1}H COSY	^{1}H-^{1}H correlation spectrometry
HMBC	heteronuclear multiple bond connectivity
HMQC	heteronuclear single quantumn connectivity
HPLC	high-performance liquid chromatography
K-Pi buffer	potassium phosphate buffer

MeCN	acetonitrile
Me_2CO	acetone
MeOH	methanol
MIC	minimum inhibitory concentration
MTPA	α-methoxy-α-(trifluoromethyl)phenylacetic acid
NADH	nicotinamide adenine dinucleotide
NADPH	nicotinamide adenine dinucleotide phosphate
NaOAc	sodium acetate
NMR	nuclear magnetic resonance
NOE	nuclear overhauser effect
NOESY	NOE correlated spectroscopy
PCR	polymerase chain reaction
SD	standard deviation
SDS-PAGE	sodium dodecyl sulfate - polyaclylamidegel electrophoresis
Si	silica
UV	ultraviolet

CHAPTER 1
GENERAL INTRODUCTION

The fungi are a highly diverse kingdom of eukaryotic microbes. The large kingdom includes the numerous molds found on decaying vegetation and the unicellular yeasts abundant on the sugary surface of ripe fruit. There are also the water-molds often seen on dead, floating fish. Mildews, smuts, rusts and many other plant pathogens are fungi. Further, there are the larger fungi: toadstools, bracket polypores, and the puff-balls and stink-horns so common in the woods in autumn. The lichens are also fungi.[1)]

Fungal plant diseases are more prevalent among cultivated crop plants, and they're more dangerous. Since cultivated crop plants are usually grown in stands of a single cultivar or variety of a species and they are all genetically identical, when a crop plant is susceptible to a fungal plant disease, all of the plants in the stand will be susceptible. Thus plant diseases caused by plant pathogens are serious problems in agriculture all over the world.

Protecting crops from fungal and other diseases also plays a key role in the widespread efforts to meet the increasing food and feed demands of a rising human population. Synthetic fungicides can effectively control some of the plant pathogens, but such fungicides may be highly toxic to non-target organisms and may also remain too long in the environment. Today, the standards to be met by new agrochemicals are very high with regard to efficiency and ecological safety.[2)]

Fungal secondary metabolites are compounds that are generally produced in a phase subsequent to growth, and they are not essential intermediaries of the central

metabolism. They often have an unusual chemical structure and are found as mixtures of closely related chemicals.[3)] In general, fungal secondary metabolites are nonessential to life, although they are important to the fungi that produce them. The filamentous fungi are proficient and copious producers of secondary metabolites. Phytopathogenic fungi also produce diverse secondary metabolites that show phytotoxic and/or antimicrobial activity and play important roles in their infection and colonization in plants.

To fully elucidate the mechanisms of infection and colonization by plant pathogens, it is necessary to identify the molecules involved in the pathogenesis. The accumulation of knowledge of such molecular infection mechanisms by plant pathogens would certainly contribute to the development of effective new and eco-friendly methods for protecting plants from many plant diseases. At the same time, such molecules could provide lead structures for agrochemicals.

This dissertation consists of four chapters. Chapter 1, this chapter, is an introduction to the general concepts and the purpose of this research. Chapter 2 focuses on the biosynthesis of phytotoxins in a phytopathogenic fungus. The conversions of deoxyradicinin to radicinin and of radicinin to 3-epi-radicinin in the cell-free system of Bipolaris coicis and the enzymes involved in these conversions are described in this chapter. Chapter 3 deals with the isolation and structural elucidation of the antimicrobial metabolites produced by a soil-born phytopathogenic fungus. The structures of new 3-O-alkyl-4a,10a-dihydrofusarubins produced by Fusarium sp. Mj-2 and their antimicrobial activities are described. Chapter 4 explains the conclusions drawn from this research and extends to speculation about future research topics.

References

1. Ingold, CT, Hudson HJ, 1993, "The Biology of Fungi. Sixth Edition," Chapman & Hall, London UK.

2. Anke T, Thines E, 2005, "Fungal metabolites as lead structures for agriculture," p. 45-58 in "Exploitation of Fungi" edited by Robson GD, van West P, Gadd GM, Cambridge University Press, Cambridge UK.

3. Hawksworth DL, Kirk PM, Sutton BC, Pegler DN, 1995, "Ainsworth & Bisby's Dictionary of The Fungi 8th Edition," CAB INTERNATIONAL, Oxon UK.

CHAPTER 2
BIOSYNTHESIS OF THE PHYTOTOXIN RADICININ IN PHYTOPATHOGENIC FUNGUS

2.1 Introduction

Radicinin (**3**) (Fig. 2-1) is a phytotoxic and antibiotic metabolite produced by some phytopathogenic fungi. It was first isolated from *Stemphylium radicinum* in the 1950s,[1] and since then has been reported to be produced by several fungal species, *Cochliobolus lunatus*,[2] *Alternaria chrysanthemi*,[3] *Alternaria helianthi*,[4] *Phoma andina*,[5] *Curvularia* sp.,[6] *Alternaria radicina* and *Alternaria petroselini*.[7] It shows phytotoxicity, for example, killing roots of *Lepidium sativum*,[8] browning and causing a loss of viability in *Nicotiana tabacum*,[9] as well as producing necrotic lesions in *Coix lachryma-jobi*[10] and inhibiting root growth in carrot seedlings.[11] The structure of radicinin (**3**) except for its stereochemistry, was determined by Grove[12] on the basis of chemical and spectroscopic evidence. Its absolute stereochemistry was inferred from the CD spectrum of the 3,4-bis-*O*-*p*-chlorobenzoyl derivative of radicinol by Nukina and Marumo based on the dibenzoate exciton chirality rule,[2] and this was supported by an X-ray crystallographic experiment with its 4-*O*-*p*-bromobenzoyl ester by Robeson et al.[13] The β-oxygenated a-pyrone moiety of radicinin (**3**) is not unusual among natural products. Its biosynthesis has been studied by some researchers. Radioactive tracer experiments by Grove[14] demonstrated that it is synthesized from two different polyketide chains originating from acetate and malonate. Other research groups confirmed this using ^{13}C labeled compounds.[15, 16] Although it has been assumed that the direct precursor of radicinin (**3**) is deoxyradicinin (**1**), there has been no experimental data to support this until now.

Formation of deoxyradicinin (**1**) through an uncommon condensation of two polyketide chains, cyclization and ring-cleavage was demonstrated by incorporation studies with ^{13}C-labeled acetates and a ^{2}H-labeled one.[17)]

The *Bipolaris coicis* H13-3 used in this study is a plant pathogen causing serious leaf blight on Job's tears (*Coix lachryma-jobi*), and Nakajima et al.[10)] reported that radicinin (**3**), 3-*epi*-radicinin (**4**), 3-*epi*-radicinol (**5**) and its epoxide (**6**) were produced by this fungus. Their structures suggested a biosynthetic relationship between these metabolites shown in Fig. 2-1. In this scheme, both radicinin (**3**) and 3-*epi*-radicinin (**4**) are synthesized from deoxyradicinin (**1**), which was isolated from the plant pathogen *A. helianthi* together with radicinin (**3**); 3-*epi*-radicinin (**4**) is then reduced to 3-*epi*-radicinol (**5**), which is oxidized to 3-*epi*-radicinol epoxide (**6**).

In this work, the hypothesis shown in Fig. 2-1 was examined by a precursor administration experiment and a cell-free approach with deoxyradicinin (**1**) and

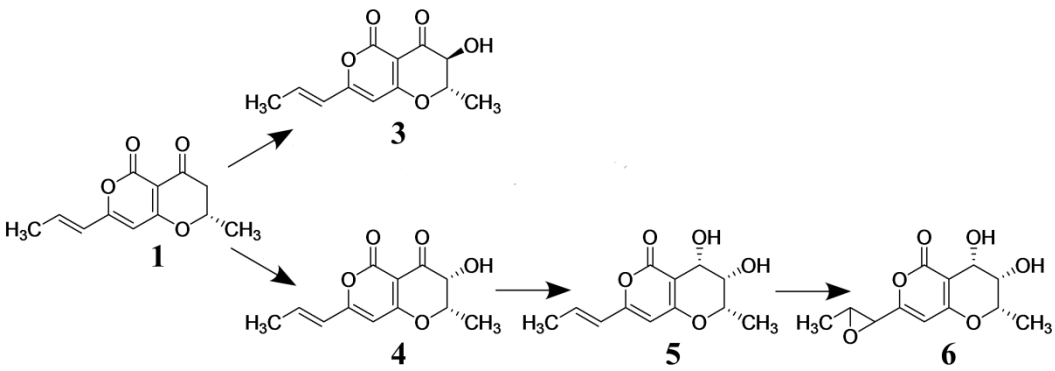

Fig. 2-1. Proposed processes for formation of radicinin (**3**) and 3-*epi*-radicinin (**4**) from deoxyradicinin (**1**) and transformation of 3-*epi*-radicinin (**4**) to the metabolites (**5** and **6**) by *Bipolaris coicis* H-13-3.

radicinin (**3**). The former was not commercially available, and a sufficient amount of deoxyradicinin (**1**) could not be obtained from *B. coicis* H13-3. Thus deoxyradicinin (**1**) was synthesized according to the reported methods.[18, 19)]

.

2.2 Feeding experiment with deoxyradicinin and radicinin

To confirm the conversion of deoxyradicinin (**1**) to radicinin (**3**) and the latter to 3-*epi*-radicinin (**4**), deoxyradicinin (**1**) and radicinin (**3**) were administered to the fungus separately. The deoxyradicinin (**1**) was synthesized from 4-methoxy-6-methyl-2*H*-pyran-2-one (**7**) according to the reported literature[10)], and the synthetic scheme is shown in Fig. 2-2.

Since the final product was a mixture of deoxyradicinin (**1**) and its C-2 epimer (**2**), they were separated via chiral HPLC. The overall yield of compounds **1** and **2** from

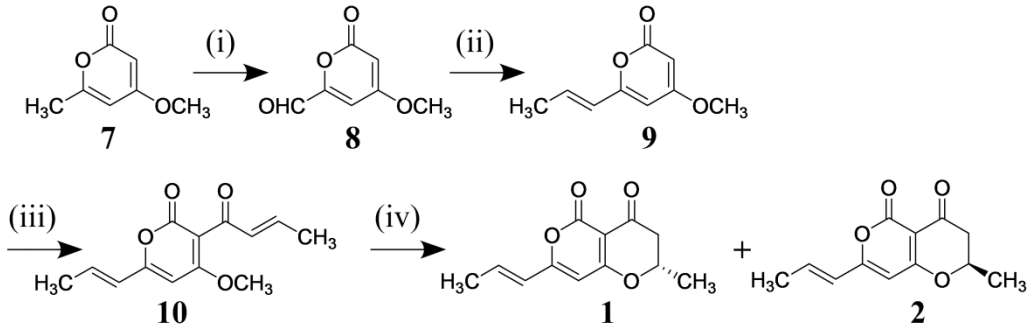

Fig. 2-2. Synthesis of deoxyradicinin (**1** and **2**). Reagents and conditions: (i) SeO_2, dioxane, 160˚C; (ii) ethyl triphenyl phosphonium bromide, sodium bis(trimethylsilyl) amide, DMF; (iii) $TiCl_4$, crotonoyl chloride, CH_2Cl_2; (iv) $TiCl_4$, CH_2Cl_2.

compound **7** was 1.2% and 1.5%, respectively. To determine which compound has the same stereochemistry as the natural product, the optical rotation of each compound was measured as –82° for compound **1** and +90° for compound **2**. To our knowledge, optical rotation of deoxyradicinin (**1**) isolated from the filamentous fungus has not been reported, and I therefore compared the optical rotation of the synthetic compounds with $[\alpha]_D$ –125° of radicinin (**3**), $[\alpha]_D$ –105° of 3-*epi*-radicinin (**4**) and $[\alpha]_D$ –19° of 3-*epi*-radicinol (**5**). From its negative optical rotation, (–)-deoxyradicinin (**1**) has the same stereochemistry as radicinin (**3**) produced by this fungus. The optical purity of compounds **1** and **2** was determined to be 94.4% ee and 96.6% ee, respectively, using chiral HPLC. The radicinin (**3**) used in the precursor administration experiment was isolated from the culture filtrate of the fungus *B. coicis* H13-3 grown on malt extract medium. Its optical purity was confirmed by analysis of the NMR spectrum of its (–)-MTPA ester, in which no resonance due to the (–)-MTPA ester of the enantiomer was detected. Thus, it was concluded that radicinin (**3**) isolated from the fungus was optically pure.

Compounds **1** and **2** were administered to the fungus separately, and the conversion products were analyzed by HPLC. As shown in Fig. 2-3B, the amount of radicinin (**3**) (27.6 nmol/L) detected, when compound **1** was administered, was about eight times more than that of the control (3.4 nmol/L). Additionally, the amount of 3-*epi*-radicinin (**4**) also increased as compared to the control. There are two possible explanations for the increase in the amount of 3-*epi*-radicinin (**4**). One is that (–)-deoxyradicinin (**1**) was hydroxylated to be 3-*epi*-radicinin (**4**) directly and the other is that radicinin (**3**) produced from (–)-deoxyradicinin (**1**) was epimerized at C-3 to be 3-*epi*-radicinin (**4**). By contrast, administration of (+)-deoxyradicinin (**2**) caused no significant increase in

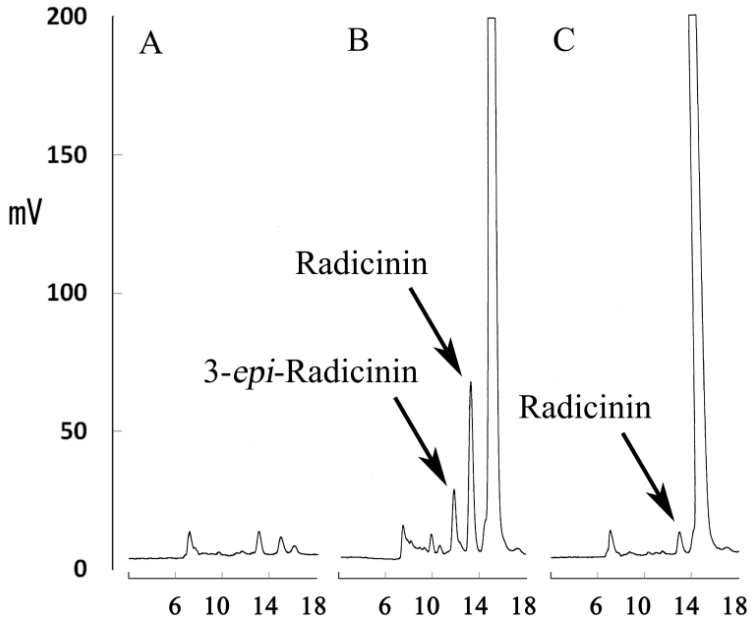

Fig. 2-3. HPLC profiles of the products converted from deoxyradicinin by *Bipolaris coicis* H13-3. (A) Control, (B) (–)-Deoxyradicinin, (C), (+)-Deoxyradicinin.

either the amounts of radicinin (**3**) or of 3-*epi*-radicinin (**4**) compared with the control (Fig. 2-3C). This supports the fact that compound **1** has the same stereochemistry at C-2 as radicinin (**3**) produced by *B. coicis*, but compound **2** does not.

To examine the biogenetical origin of 3-*epi*-radicinin (**4**), radicinin (**3**) was administered to the fungus, and the conversion products were analyzed by HPLC. As shown in Fig. 2-4, when radicinin (**3**) was administered, there was about a 4-fold increase in the amount of 3-*epi*-radicinin (**4**) (3.5 nmol/L) detected by HPLC compared with the control (0.9 nmol/L). These results indicated that (–)-deoxyradicinin (**1**), not (+)-deoxyradicinin (**2**), is a direct precursor of radicinin (**3**) and also that the fungus have an epimerizing enzyme which catalyzes the conversion of radicinin (**3**) to 3-*epi*-radicinin (**4**).

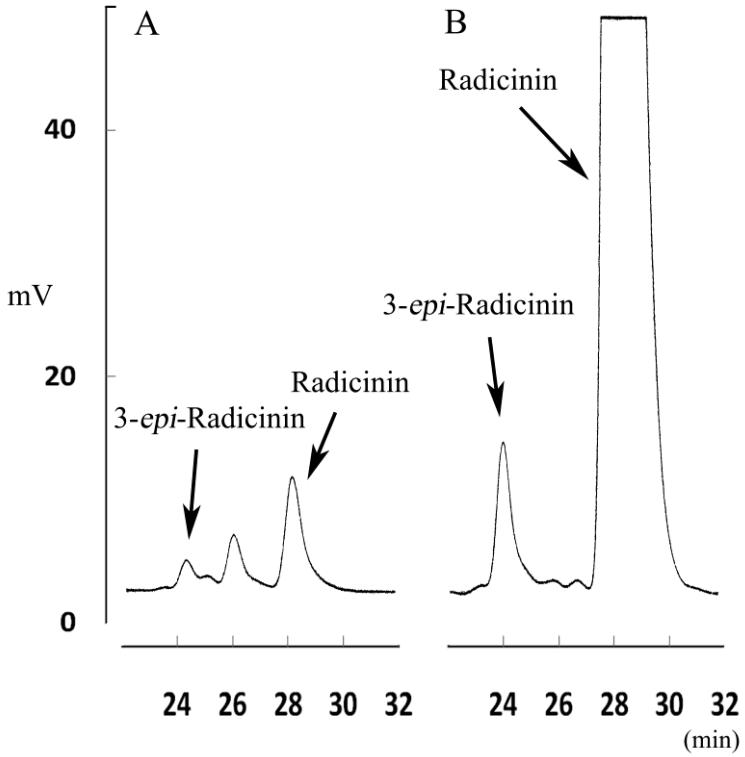

Fig. 2-4. HPLC profiles of the products converted from radicinin by *Bipolaris coicis* H13-3. (A) Control, (B) Radicinin.

In our previous report[10], a biosynthetic relationship was proposed between radicinin (**3**) and its analogues based on their structural features. The present result obtained from the feeding experiments indicates that radicinin (**3**) is synthesized from an anticipated precursor, deoxyradicinin (**1**). Furthermore, a small amount of deoxyradicinin (**1**) was produced by *B. coicis*, suggesting that the deoxyradicinin (**1**) biosynthesized is rapidly converted to radicinin (**3**) or to the following biosynthetic product, and thus ostensible amount of deoxyradicinin (**1**) is extremely small in amount at any time.

2.3 Enzyme activity of deoxyradicinin monooxygenase and radicinin epimerase

To confirm the conversion of deoxyradicinin (**1**) to radicinin (**3**) as indicated by precursor administration, the experiment using a cell-free system prepared from *B. coicis* H13-3 was carried out as follows. Incubation of (–)-deoxyradicinin (**1**) with the crude cell free extract, in the presence of co-enzymes (NAD^+, $NADP^+$, NADH and NADPH 20 mM respectively), for 2 h gave rise to the enzymatic formation of radicinin (**3**) (Fig. 2-5). Next, the crude cell free extract was divided into cytosolic and microsomal fractions. When (–)-deoxyradicinin (**1**) was incubated with the cytosolic fraction in the presence of co-enzymes (NAD^+, $NADP^+$, NADH and NADPH), the amount of radicinin (**3**) after 2-h incubation increased remarkably, but when incubated with the microsomal fraction, no significant formation of radicinin (**3**) was detected.

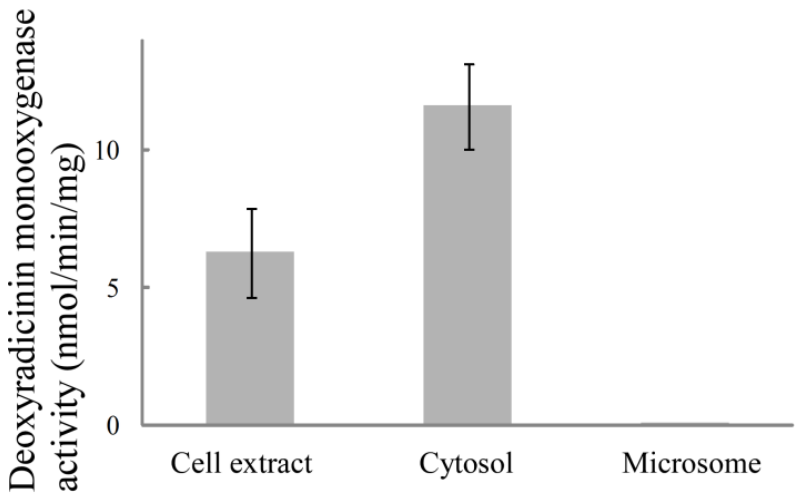

Fig. 2-5. Deoxyradicinin monooxygenase activity to convert (–)-deoxyradicinin (**1**) to radicinin (**3**) in the cell-free extract, cytosolic and microsomal fractions. Data presented is mean of three replicates and SD.

(+)-Deoxyradicinin (**2**) was also incubated with the cytosolic fraction or the microsomal fraction in the presence of co-enzymes (NAD^+, $NADP^+$, NADH and NADPH), but, in both cases, no remarkable increases in the amount of radicinin (**3**) in the 2-h incubation extracts were observed.

Deoxyradicinin 3-monooxygenase activity was measured under various conditions with the cytosolic fractions. The optimum temperature for the enzyme activity was determined by comparing the reaction rates at 25–45 °C at pH 7.0. The optimum pH for the enzyme activity was determined by comparing the reaction rates at pH 4–9 at 35 °C. (Fig. 2-6) demonstrates that the reaction was catalyzed most effectively by the monooxygenase at 35 °C, pH 7.0. The monooxygenase prefers NAD^+ to other co-enzymes (Fig. 2-7).

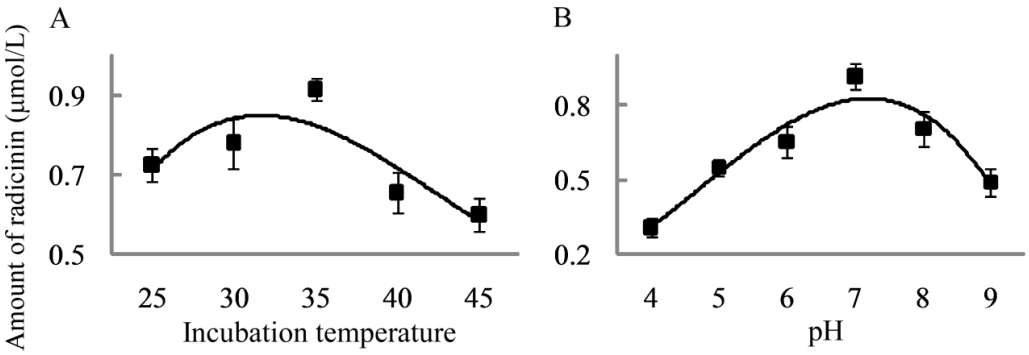

Fig. 2-6. Effect of incubation temperature and pH on activity of the enzyme catalyzing the conversion of (–)-deoxyradicinin (**1**) to radicinin (**3**). Cytosol fraction was used to determine its optimal temperature and pH in the range of 20 to 50 °C at pH 7.0, and of 4.0 to 9.0 at 35 °C. The amount of radicinin formed was measured by HPLC. Data presented is the mean of three replicates and SD.

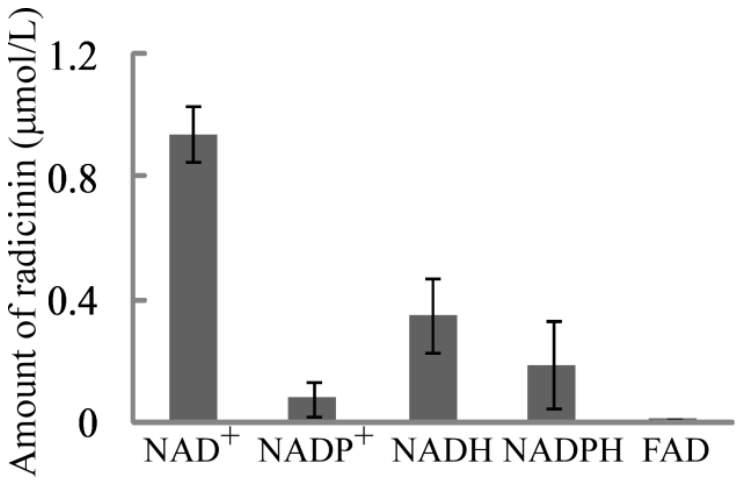

Fig. 2-7. Effect of addition of co-enzyme to the enzyme assay solution on formation of radicinin (**3**) from (–)-deoxyradicinin (**1**). The cytosolic fraction was used for the reaction with co-enzymes, and the reaction was carried out at 35 °C and at pH7.0. The amount of radicinin formed was measured by HPLC using the experimental procedure described above. All experimental analyses were carried out in a minimum of three independent complexes for each condition.

The molecular weight of the monooxygenase was determined to be 130–184 kDa by gel filtration column chromatography. Although it was suggested in a previous paper that the enzyme catalyzing this reaction was cytochrome P450 monooxygenase[10], the enzyme activity for the conversion of deoxyradicinin (**1**) to radicinin (**3**) was distributed in the cytosolic fraction and not in the microsomal fraction. The monooxygenase is therefore, a soluble protein present in the cytoplasm. The enzyme that catalyzes the hydroxylation like this was classified as oxidoreductase, and is activated in the presence of NAD^+. Thus deoxyradicinin 3-monooxygenase belongs to a monooxygenase group such as EC 1.14.13.

To investigate the metabolism of radicinin (**3**) and the origin of 3-*epi*-radicinin (**4**),

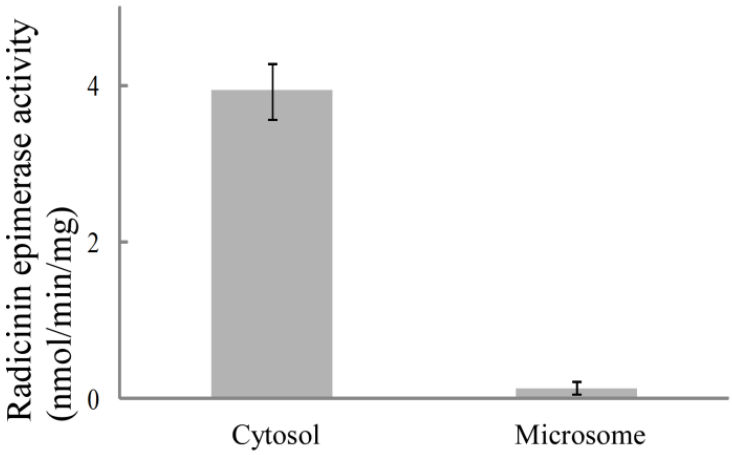

Fig. 2-8. Radicinin epimerase activity to epimerize radicinin (**3**) to 3-*epi*-radicinin (**4**) in the cytosolic and microsomal fractions. Data presented is the mean of three replicates and SD.

radicinin (**3**) was incubated with the cytosolic or microsomal fraction in the presence of co-enzymes (NAD^+, $NADP^+$, NADH and NADPH) for 30 min (Fig. 2-8). Incubation of radicinin (**3**) with the cytosolic fraction caused an increase in 3-*epi*-radicinin (**4**), but no increase of 3-*epi*-radicinin (**4**) was observed when incubating with the microsomal fraction. No 3-*epi*-radicinin (**4**) was detected when incubating radicinin (**3**) with distilled water in place of the cytosolic or the microsomal fraction, indicating that radicinin (**3**) does not racemize at detectable rate without enzyme.

The radicinin epimerase that catalyzes the reaction of radicinin to 3-*epi*-radicinin (**4**) was purified with ammonium sulfate fractionation and several chromatographic processes by monitoring enzyme activity (Table 2-1). To characterize the epimerase, radicinin (**3**) was incubated with this purified enzyme under several conditions, demonstrating that the highest activity of the epimerase was found at 30–35 °C and pH

7.0–9.0 (Fig. 2-9), and that the epimerase did not require any co-enzyme for this conversion. The molecular weight of the epimerase was determined to be 52 kDa based on its gel filtration chromatographic behavior. The fractions from the 2nd Mono Q HR 5/5 column chromatography were characterized by SDS–PAGE analysis and enzyme assay. A major band corresponding to 28-kDa on SDS–PAGE is in accordance with the enzyme activity, indicating that the epimerase is homodimeric in its native condition (Fig. 2-10).

Table 2-1. Purification of radicinin epimerase from *Bipolaris coicis* H 13-3. Total protein was measured by Bradford protein assay. Total activity was calculated from the reaction product monitoring by HPLC. Total specific activity was assayed spectrophotometrically by measuring the absorbance of 3-*epi*-radicinin in the enzymatic assay at 280 nm.

Purification step	Total protein (mg)	Total activity (nmol/min)	Specific activity (nmol/min/mg)	Purification Fold	Recovery (%)
Cytosol	262.0	1035.0	4.0	1.0	100.0
DE-52	40.6	230.0	5.7	1.4	22.3
Phenyl Sepharose	13.9	140.0	10.1	2.6	14.0
Superdex	2.12	38.7	18.3	4.5	3.7
1st MonoQ	0.22	13.7	62.3	15.8	1.3
2nd MonoQ	0.04	9.1	228.0	57.7	0.9

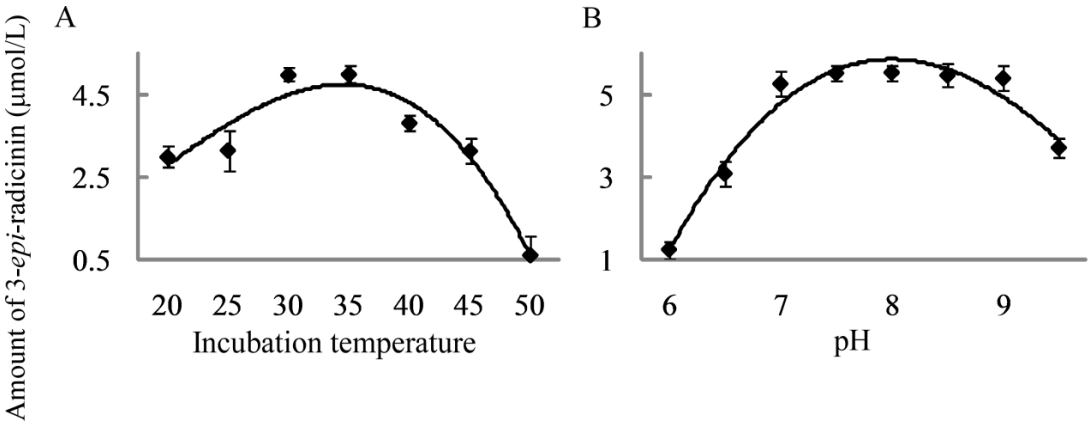

Fig. 2-9. Effect of incubation temperature and pH on activity of the enzyme that catalyzes the conversion of radicinin (**3**) to 3-*epi*-radicinin (**4**). The purified enzyme was used to determine its optimal temperature and pH in the range of 20 to 50°C at pH 8.0, and of 6.0 to 9.5 at 35°C. The amount of 3-*epi*-radicinin formed was measured by HPLC. Data presented is the mean of three replicates and SD.

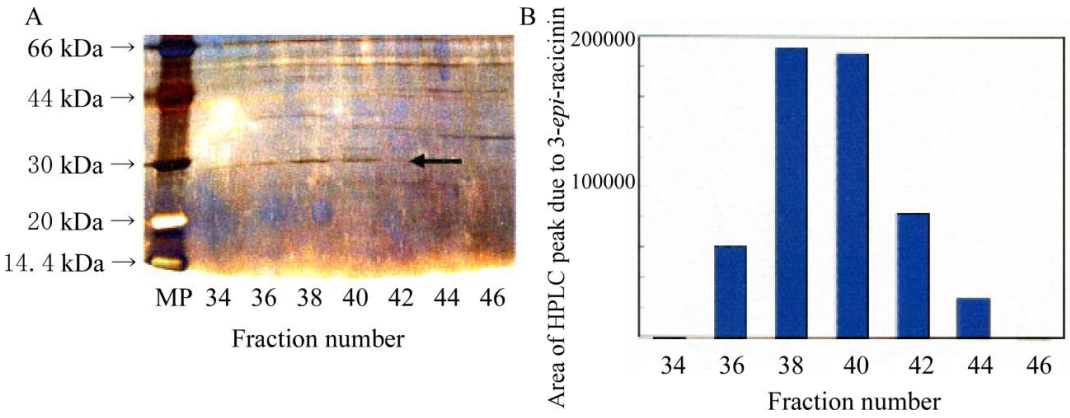

Fig. 2-10. SDS-PAGE analysis and the enzyme activity of 2nd Mono Q fractions. (A) SDS-PAGE of the fractions 34-46 from the 2nd Mono Q column chromatography and marker proteins (MP). Arrow indicates the enzyme band. (B) Amount of 3-*epi*-radicinin formed when radicinin was incubated with each 2nd Mono Q fraction. 3-*epi*-Radicinin formed was extracted with EtOAc and analyzed by HPLC.

To ascertain whether the epimerase catalyzes the inverse reaction, the isolated epimerase was incubated with 3-*epi*-radicinin (**4**). HPLC analysis of the products indicated formation of radicinin (**3**) from 3-*epi*-radicinin (**4**) (data not shown), demonstrating that this reaction was reversible. The enzyme activity was inhibited by copper sulfate and iodoacetic acid (data not shown), suggesting that radicinin epimerase is a SH enzyme. Most epimerization enzymes that have been discovered so far utilize carbohydrates, amino acids, hydroxyl acids and their derivatives as substrates[20-23]. However, no epimerization enzymes involved in secondary metabolism have been found until now. The epimerase did not need any co-enzymes for the reaction, indicating that the reaction proceeds through keto-enol tautomerization. Thus, radicinin epimerase should belong to the tautomerase group such as the EC number of 5.3.2. The toxicity of radicinin (**3**) for *Coix lachryma-jobi L*. was ten times higher than 3-*epi*-radicinin (**4**), and hence it was assumed that radicinin epimerase regulated the pathogenicity of the fungus to the plants.

Previously, Nakajima et al. proposed that the same enzyme catalyzes the conversions of deoxyradicinin (**1**) to radicinin (**3**) and also to 3-*epi*-radicinin (**4**).[10] Actually, the precursor administration experiment with deoxyradicinin (**1**) showed formation of not only radicinin (**3**), but also 3-*epi*-radicinin (**4**). At the same time, however, I established that the enzyme in the cytosolic preparation from *B. coicis* H13-3 catalyzes reaction of radicinin (**3**) to 3-*epi*-radicinin (**4**). This epimerization was reversible and a new metabolic fate of radicinin (**3**). From these results, a biosynthesis and metabolism scheme for radicinin (**3**) was deduced, as shown in Fig. 2-11. First, deoxyradicinin (**1**) is converted to radicinin (**3**) by stereospecific hydroxylation at C-3. Then, radicinin epimerase catalyzes epimerization of radicinin (**3**) at C-3 to

3-*epi*-radicinin (**4**) reversibly. The direct conversion of deoxyradicinin (**1**) to 3-*epi*-radicinin (**4**) could not be confirmed in this study. Finally, 3-*epi*-radicinin is probably converted to 3-*epi*-radicinol (**5**) by stereospecific reduction at C-4, followed by epoxidation of the side chain in 3-*epi*-radicinol (**5**). In this study, the key enzyme that catalyzes the reaction of deoxyradicinin (**1**) to radicinin (**3**) could not be isolated, probably because of enzyme instability.

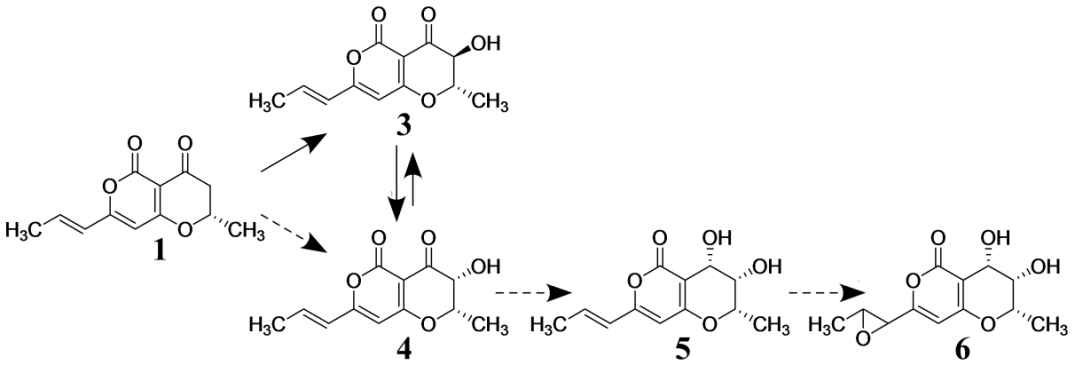

Fig. 2-11. Biosynthesis of radicinin (**3**) from (–)-deoxyradicinin (**1**) and conversion of radicinin to 3-*epi*-radicinin (**4**). Solid arrows show the pathways established in this research, and dashed arrows show the unproven pathways.

2.4 Experiments

2.4.1 General experimental procedures

NMR spectra were recorded in $CDCl_3$ on a JEOL JNM-ECP 500 spectrometer. NMR chemical shifts were referenced to $CDCl_3$ (δ_H 7.26, δ_C 77.0). Mass spectra were obtained with a JEOL AX-505 spectrometer. Optical rotations were determined with a Horiba SEPA-200 high sensitive polarimeter. A Shimadzu LC-6A liquid chromatography system was used for HPLC analysis. In the precursor administration

experiment and the enzyme assay for the conversion of deoxyradicinin (**1**) to radicinin (**3**), HPLC was performed using a DAISOPAK SP-120-5-ODS-AP column (6 x 150 mm, DAISO Co., Ltd., Osaka Japan), MeOH–H_2O–AcOH (100:99:1, v/v/v) as solvent at a flow rate of 0.5 mL/min, monitoring at 280 nm. In the enzyme assay for the conversion of radicinin (**3**) to 3-*epi*-radicinin (**4**), HPLC was carried out using a DAISOPAK SP-250-10-ODS-AP column (10 x 250 mm), MeOH–H_2O–AcOH (100:99:1, v/v/v) as solvent at a flow rate of 0.5 mL/min, and monitoring at 280 nm. Silica gel flash column chromatography was carried out by use of Wakogel FC-40 (Wako Pure Chemical Industries, Ltd., Osaka, Japan). Protein concentrations were determined with Bradford reagent (Sigma–Aldrich) using BSA as a standard.

2.4.2 Fungal strain

The strain H13-3 of *B. coicis* was used in the experiments. *B. coicis* H13-3 was maintained on potato dextrose agar slants.

2.4.3 Isolation of radicinin

The fungus was grown without shaking at 24˚C for 14 days in the dark in a 500 mL conical flask containing liquid medium (200 mL x 5) made up of glucose (30 g/L), peptone (3 g/L) and an extract from 50 g/L of malt and H_2O. The culture filtrate was acidified to pH 2.0 with HCl, and the metabolites in the culture filtrate were extracted with EtOAc (500 mL x 3). The EtOAc extract was dried over Na_2SO_4 and evaporated. The residue (270 mg) was applied to a Si gel column (Daisogel IR-60, 18 x 180 mm, DAISO, Co., Ltd.), and the column was washed with 1500 mL of Me_2CO–*n*-hexane (1:9,v/v), then developed successively with 750 mL each of Me_2CO–*n*-hexane (2:8, 3:7

and 4:6, v/v). Fractions 3 and 4 eluted by Me_2CO–*n*-hexane (3:7, v/v) were combined and evaporated. Recrystallization of the residue (34 mg) from MeOH afforded radicinin (**3**) as colorless needles (6 mg): δ_H 6.93 (1H, dq, *J* = 15.5, 7.0 Hz, 20-H), 6.02 (1H, dq, *J* = 15.5, 1.7 Hz, 10-H), 5.83 (1H, s, 8-H), 4.36 (1H, dq, *J* = 12.4, 6.0 Hz, 2-H), 3.97 (1H, d, *J* = 12.4 Hz, 3-H), 1.96 (3H, dd, *J* = 7.0, 1.7 Hz, 3'-H), 1.64 (3H, d, *J* = 6.0 Hz, 2-Me); δ_C ($CDCl_3$) 188.7, 176.0, 164.4, 156.8, 141.0, 122.6, 98.1, 97.2, 80.0, 72.0, 18.8, 18.1, CI-MS (*iso*-butane, probe), 200 eV, *m/z* 237 ($[M+H]^+$, 100%).

2.4.4 Synthesis of deoxyradicinin

2.4.4.1 6-Formyl-4-methoxy-2H-pyran-2-one (8)

The mixture of 4-methoxy-6-methyl-2*H*-pyran-2-one (**7**; 500 mg, Sigma–Aldrich, Inc.), SeO_2 (1.2 g, Kanto Chemical Co., Inc., Tokyo, Japan) and anhydrous dioxane (5 mL) in a sealed tube was heated at 160˚C (outside) and stirred vigorously. After 3 h, the precipitate was removed by filtration and washed with dioxane. The latter was removed by evaporation in vacuo to afford a residue, which was poured into brine (100 mL). The resulting product was extracted with EtOAc (100 mL x 3) with the EtOAc solubles combined. After drying over Na_2SO_4, the extract was evaporated to dryness. The residue was purified by Si gel flash CC. The column (20 x 150 mm) was developed successively with 300 mL of Me_2CO–*n*-hexane (3:7, 4:6 and 1:1 v/v), respectively. Compound **8** (362 mg) was eluted with Me_2CO–*n*-hexane (4:6, v/v): δ_H 9.48 (1H, s, 7-H), 6.63 (1H, d, *J* = 2.3 Hz, 5-H), 5.70 (1H, d, *J* = 2.3 Hz, 3-H), 3.82 (3H, s, 8-H); EI-MS, 70 eV, *m/z* 154 (M^+, 22%), 125 (100), 69 (20), and 59 (15).

2.4.4.2 4-Methoxy-6-[(*E*)-1-propenyl]-2*H*-pyran-2-one (9)

Ethyltriphenylphosphoniumbromide (1.2 g, Wako Pure Chemical Industries, Ltd., Osaka, Japan) was dissolved into DMF (11 mL), and then bis(trimethylsilyl) amide (3 mL, Sigma–Aldrich, Inc.) was added. Compound **8** (120 mg) in DMF (4 mL) was added and the mixture was stirred vigorously at r.t. for 3 h under N_2. The reaction mixture was poured into brine (70 mL) and extracted with EtOAc (70 mL x 3). The combined EtOAc solubles were dried (Na_2SO_4) and evaporated in vacuum to dryness. The residue was subjected to Si gel flash CC (20 x 150 mm), which was developed successively with 200 mL each of Me_2CO–*n*-hexane (5:95, 1:9, 2:8 and 3:7, v/v), respectively. Compound **9** and its *Z*-isomer were eluted with Me_2CO–*n*-hexane (1:9 and 1:4, v/v) fractions (61 mg). Heating of the crystalline mixture at 130˚C in a sealed tube under N_2 caused isomerization to give 57 mg of compound **9**: δ_H 6.68 (1H, dq, *J* = 15.5, 7.0 Hz, 8-H), 5.97 (1H, dq, *J* = 15.5, 1.5 Hz, 7-H), 5.74 (1H, d, *J* = 2.2 Hz, 5-H), 5.43 (1H, d, *J* = 2.2 Hz, 3-H), 3.80 (3H, s, 10-H), 1.88 (3H, dd, *J* = 7.0, 1.5 Hz, 9-H); EI-MS, 70 eV, *m/z* 166 (M^+, 63%), 138 (100), and 69 (38)

2.4.4.3 3-3-[(*E*)-2-butenoyl]-4-methoxy-6-[(*E*)-1-propenyl]-2*H*-pyran-2-one (10)

To a mixture of compound **9** (80 mg) and $TiCl_4$ (260 μL, Wako Pure Chemical Industries, Ltd.) in CH_2Cl_2 (1 mL), crotonoyl chloride (70 μL, Wako Pure Chemical Industries, Ltd.) was added slowly. The solution was stirred at r.t. for 20 min, and then at 45˚C for 6 h. It was then poured into brine (30 mL), and extracted with EtOAc (30 mL x 3). The EtOAc solubles were combined, dried over Na_2SO_4, and evaporated to dryness. The resulting residue was purified by Si gel flash CC (20 x 150 mm) developed successively with 100 mL each of Me_2CO in *n*-hexane (1:4, 1:3, 3:7 and 35:65 v/v).

Compound **10** (40 mg) was eluted with Me_2CO–*n*-hexane (1:4, v/v) whereas compounds **1** and **2** were eluted using Me_2CO–*n*-hexane (3:7, v/v). Separation of compounds **1** and **2** by chiral HPLC used a CHIRALPAK OD column (Daicel Chemical Industries, Ltd., 4.6 x 250 mm), eluted with EtOH-*n*-hexane (1:1, v/v) at a flow rate of 0.5 mL/min, and monitoring at 280 nm to afford compounds **2** (2.5 mg) and **1** (3.0 mg). The retention times of compounds **2** and **1** were 26.2 and 30.8 min, respectively. Compound **10**: δ_H 1.85 (3H, dd, *J* = 7.0, 1.4 Hz, 9-H), 1.87 (3H, dd, *J* = 7.0, 1.4 Hz, 14'-H), 3.82 (3H, s, 10-H), 5.94 (1H, s, 5-H), 5.97 (1H, dq, *J* = 15.5, 1.4 Hz, 7-H), 6.40 (1H, dq, *J* = 15.5, 1.4 Hz, 12-H), 6.82 (2H, m, 8, 13-H); EI-MS, 70 eV, *m/z* 234 (M^+, 100%), 193 (80), 165 (48), and 138 (32).

2.4.4.4 Deoxyradicinin (1)

A mixture of compound **10** (40 mg), $TiCl_4$ (90 μL) and CH_2Cl_2 (1 mL) was stirred at 45˚C for 3 h. It was then poured into brine (30 mL), extracted with EtOAc (30 mL x 3). The organic layer was washed with brine (100 mL x 3). The combined EtOAc extracts were dried (Na_2SO_4) and evaporated to dryness, with the residue was subjected to Si gel flash CC (20 x 150 mm) developed successively with 100 mL each of Me_2CO-*n*-hexane (1:4, 1:3, 3:7 and 35:65, v/v). Compounds **1** and **2** were eluted with Me_2CO-*n*-hexane (3:7, v/v), and separated by chiral HPLC as above to afford compounds **2** (1.8 mg) and **1** (2.5 mg). Compound **1**, **2**: δ_H 6.86 (1H, m, 20-H), 5.95 (1H, dq, *J* = 15.5, 1.8 Hz, 10-H), 5.76 (1H, s, 8-H), 4.67 (1H, m, 2-H), 2.59 (2H, m, 3–H), 1.88 (3H, dd, *J* = 7.3, 1.4 Hz, 3'-H), 1.46 (3H, d, *J* = 5.6 Hz, 2-Me); δ_C 186.2, 176.6, 163.8, 156.7, 138.9, 124.0, 100.7, 99.1, 77.6, 44.3, 20.4, 18.6; EI-MS, 70 eV, *m/z* 220 (M^+, 100%), 205 (50), and 177 (59). Compound **1**: $[\alpha]_D$ –82° (*c* 0.1, $CHCl_3$) Compound **2**:. $[\alpha]_D$ +90˚ (*c* 0.1,

$CHCl_3$).

2.4.5 Precursor administration

The fungus was grown on medium (500 μL) containing 15 g/L of malt extract broth (Difco Laboratories Inc.) in a test tube (8 x 75 mm) without shaking at 24 °C for 7 days in the dark. Then the medium was removed aseptically from the tube with fungal mats washed with 100 mM K-Pi buffer, pH 7.0. The fungus was incubated in 500 μL of the same buffer at 24˚C for 3 days in the dark. After incubation, the buffer was removed from the tube aseptically and the fungal mats were washed with buffer. Then, new buffer (500 μL) was introduced into the tube and DMSO (50 μL) containing precursor (0.05 mg) was added to the buffer. After 5 days incubation, the fungal mat was removed and the remaining buffer was extracted with EtOAc (100 μL x 3). The EtOAc extracts were combined, air-dried overnight, redissolved in MeOH and analyzed by HPLC as described in Section 2.4.1. Retention times of compounds **1**, **3** and **4** were 15.8, 13.5 and 11.8 min, respectively.

2.4.6 Preparation of cell-free extract

The grown mycelia were homogenized with sea sand, a mortar and pestle in 50 mM K-Pi buffer, pH 7.0 at 4 °C. The homogenate was centrifuged at 2500*g* for 10 min at 4 °C. The supernatant was centrifuged at 19,000*g* for 15 min at 4 °C to yield the cell-free extract. The extract thus obtained was then subjected to ultracentrifugation at 30,000*g* for 180 min at 4 °C to afford cytosolic and microsomal fractions. The microsomal precipitates were suspended in 50 mM K-Pi buffer, pH 7.0, and used for the experiments. Glycerol was added to each fraction up to 15% (v/v), and fractions were

maintained at –80 °C until use.

2.4.7 Enzyme activity

The following method was used to detect deoxyradicinin monooxygenase or radicinin epimerase activity in the cell extract, cytosolic and microsomal fractions. The crude enzyme preparation (10 μL) was incubated at 35 °C for 2 h or 30 min with 2 μL of 20 mM substrate in MeOH, 3 μL of co-factor solution (containing 20 mM each of NAD^+, $NADP^+$, NADH and NADPH), 35 μL of 70mM K-Pi buffer, pH 7.0. During purification of epimerase, 3 μL of buffer was used in place of 3 μL of co-factor solution in the enzyme assay. After incubation, the reaction mixture was extracted with EtOAc (100 μL x 3). The combined EtOAc solution was air-dried overnight, dissolved in the MeOH, and analyzed by HPLC described in Section 2.4.1. In the HPLC analysis for the conversion of deoxyradicinin (**1**) to radicinin (**3**), their retention times were 15.8 and 13.5 min and in the HPLC analysis for conversion of radicinin (**3**) to 3-*epi*-radicinin (**4**), those were 28.5 and 24.0 min. The crude enzyme solution usually contained radicinin (**3**) and 3-*epi*-radicinin (**4**). Thus EtOAc was added first to the enzyme cocktail prior to substrate and then substrate was added. The mixture was extracted with EtOAc without incubation. The EtOAc extract was analyzed by HPLC to afford the initial amount of the products in the enzyme solution. The true amount of the product formed by the enzyme preparation was obtained by subtracting initial amount from amount after enzyme reaction. To determine the effect of pH on enzyme activity and stability, 0.2 M NaOAc buffer was used for pH 4.0 to 5.0, 0.2 M K-Pi buffer for pH 6.0 to 8.0 and 0.2 M Tris-HCl buffer for pH 7.0 to 9.5. One milli molar of phenylmethylsulfonyl fluoride in 50 mM K-Pi buffer (pH 7.0) was used for the optimum temperature determination of

the monooxygenase enzyme (Fig. 2-6), and 0.4 mM EDTA, 10 mM $MgCl_2$, 10% glycerol in 20 mM Tris–HCl buffer (pH 8.0) was used for the optimum temperature determination of the epimerase enzyme (Fig. 2-9).

2.4.8 Purification of radicinin epimerase

All procedures were conducted at 4˚C unless otherwise stated. The cytosolic fraction was loaded onto a DE52 (Whatman) column (38 x 100 mm) equilibrated with 50 mM Tris–HCl buffer (pH 7.0). The column was washed with 80 mL of buffer, followed by a linear gradient elution of 0–0.5 M NaCl in the buffer, at a flow rate of 0.6 mL/min, and each 3.0 mL was collected as one fraction. Active fractions eluted between 0.19 and 0.31 M NaCl were combined, and an equivalent amount of buffer containing 1.6 M $(NH_4)_2SO_4$ was added. The solution was loaded onto a Phenyl Sepharose CL- 4B (Sigma–Aldrich) column (9 x 90 mm). The column was washed with 0.8 M $(NH_4)_2SO_4$ buffer (80 mL), followed by a linear gradient elution of 0.8–0 M $(NH_4)_2SO_4$ in the buffer, at a flow rate of 0.6 mL/min, and each 2.0 mL fraction was collected. Active fractions eluting between 0.56 and 0.32 M were combined, loaded onto a Superdex 200 10/300 GL (GE Healthcare) column, eluted with 20 mM Tris–HCl buffer (pH 8.0) at a flow rate of 0.6 mL/min, and each 0.5 mL was collected as one fraction. Active fractions were combined and loaded onto a Mono Q HR 5/5 (Amersham) column (3.8 x 100 cm) equilibrated with 20 mM Tris–HCl buffer (pH 8.0). The column was washed with 80 ml of the same buffer, followed by a linear gradient elution of 0–0.4 M NaCl in the buffer, at a flow rate of 0.5 ml/min, and each 0.3 ml was collected as one fraction. The active fractions eluted between 0.18 and 0.23 M NaCl were combined, and the same purification with a Mono Q HR 5/5 (Amersham) column was repeated. Radicinin

epimerase was eluted at around 0.21 M NaCl (see Table 2-1 and Fig. 2-10B).

2.4.9 Determination of molecular weights of deoxyradicinin monooxygenase and radicinin epimerase

To determine the molecular weights of monooxygenase and epimerase, Superdex 200 10/300 GL CC was performed as described above with the standard proteins, thyroglobulin (670 kDa), gamma globulin (158 kDa), ovalbumin (44 kDa), myoglobin (17 kDa) and vitamin B-12 (1.35 kDa).

2.4.10 SDS-PAGE

After reduction with 2-mercaptoethanol, the relative molecular mass of the purified enzyme was determined by sodium dodecyl sulfate–polyacrylamide gel electrophoresis (SDS–PAGE) on 10% polyacrylamide gels at 75 mA per slab with Tris–glycine, pH 8.3, using 0.1% SDS as running buffer. Coomassie brilliant blue stain solution (CBB R-25 1 g, MeOH 100 mL, AcOH 30 mL, in D.W. 400 mL) was used to stain the enzyme. After decolorization, the gel was stained with a silver staining kit (Silver Staining II kit, Wako Pure Chemical Industries, Ltd.). LMW Marker Kit (GE Healthcare) was used as molecular marker (Fig. 2-10A).

2.5 References

1. Clarke DD, Nord FF, 1953, Radicinin: a new pigment from *Stemphylium radicinum*. *Arch. Biochem. Biophys*. **45**, 469–470.

2. Nukina M, Marumo S, 1977, Radicinol, a new metabolite of *Cochliobolus lunata*, and absolute stereochemistry of radicinin. *Tetrahedron Lett*. **37**, 3271–3272.

3. Robeson DJ, Gary GR, Strobel GA, 1982, Production of the phytotoxins radicinin and radicinol by *Alternaria chrysanthemi*. *Phytochemistry* **21**, 2359–2362.

4. Tal B, Robeson DJ, Burke BA, Aasen AJ, 1985, Phytotoxins from *Alternaria helianthi*: radicinin, and the structures of deoxyradicinol and radianthin. *Phytochemistry* **24**, 729–731.

5. Noordeloos ME, De Gruyter J, Van Eijl GW, Roeijmans HJ, 1993, Production of dendritic crystals in pure cultures of *Phoma* and *Ascochyta* and its value as a taxonomic character relative to morphology, pathology and cultural characteristics. *Mycol. Res*. **97**, 1343–1350.

6. Kadam S, Poddig J, Humphrey P, Karwowski J, Jackson M, Tennent S, Fung L, Hochlowski J, Rasmussen R, McAlpine J, 1994, Citrinin hydrate and radicinin: human rhinovirus 3C-protease inhibitors discovered in target-directed microbial screen. *J. Antibiot*. **47**, 836–839.

7. Pryor BM, Gilbertson RL, 2002, Relationships and taxonomic status of *Alternaria radicina*, *A. Carotiincultae*, and *A. petroselini* based upon morphological, biochemical, and molecular characteristics. *Mycologia* **94**, 49–61.

8. Hansen RO, 1954, Stemphylone, a root-killing substance from *Stemphylium radicinum*. *Acta Chem. Scand*. **8**, 1332–1334.

9. Canning AM, Hook I, Sheridan H, James JP, Kelly DR, 1992, Bisradicinin: a novel dimer elicited in cultures of *Alternaria chrysanthemi*. *J. Nat. Prod.* **55**, 487– 490.

10. Nakajima H, Ishida T, Otsuka Y, Hamasaki T, Ichinoe M, 1997, Phytotoxins and related metabolites produced by *Bipolaris coicis*, the pathogen of Job's tears. *Phytochemistry* **45**, 41–45.

11. Solfrizzo M, Vitti C, De Girolamo A, Visconti A, Logrieco A, Fanizzi FP, 2004,

Radicinols and radicinin phytotoxins produced by *Alternaria radicina* on carrots. *J. Agric. Food Chem*. **52**, 3655–3660.

12. Grove JF, 1964, Metabolic products of *Stemphylium radicinum*. Part I. Radicinin. *J. Chem. Soc.*, 3234–3239.

13. Robeson DJ, Strobel GA, 1982, Deoxyradicinin, a novel phytotoxin from *Alternaria helianthi*. *Phytochemistry* **21**, 1821–1823.

14. Grove JF, 1970, Metabolic products of *Stemphylium radicinum*. Part III. Biosynthesis of radicinin and pyrenophorin. *J. Chem. Soc. C: Organic*. **13**, 1860–1865.

15. Tanabe M, Seto H, Johnson L, 1970, Biosynthetic studies with carbon-13. Carbon13 nuclear magnetic resonance spectra of radicinin. *J. Am. Chem. Soc*. **92**, 2157–2158.

16. Seto H, Urano S, 1975, Revised assignment of the ^{13}C NMR spectrum of radicinin. *Agric. Biol. Chem.* **39**, 915–916.

17. Tal B, Goldsby G, Burke BA, Aasen AJ, Robeson DJ, 1988, Studies on the mechanism of polyketide-derived biosynthesis of deoxyradicinin and related metabolites of *Alternaria helianthi*. *J. Chem. Soc. Perkin Trans.* I, 1283–1287.

18. Kato K, Hirata Y, Yamamura S, 1969, Syntheses of (±)-radicinin and (±)-dihydroradicinin. *J. Chem. Soc.* (C) **15**, 1997–2002.

19. Suzuki E, Hamajima R, Inoue S, 1975, A facile synthesis of 6-conjugated 2-pyrones. *Synthesis* **3**, 192-194.

20. Mazumder R, Sasakawa T, Kaziro Y, Ochoa S, 1962, Metabolism of propionic acid in animal tissues. IX. Methylmalonyl coenzyme A racemase. *J. Biol. Chem*. **237**, 3065–3068.

21. Dahm K, Lindlau M, Breuer H, 1968, Steroid epimerase-a new enzyme of oestrogen

metabolism. *Biochim. Biophys. Acta* **159**, 377–389.

22. van der Drift L, Vogels GD, van der Drift C, 1975, Allantoin racemase: a new enzyme from *Pseudomonas* species. *Biochim. Biophys. Acta* **391**, 240–248.
23. Schmitz W, Fingerhut R, Conzelmann E, 1994, Purification and properties of an α-methylacyl-CoA racemase from rat liver. *Eur. J. Biochem*. **222**, 313–323.

CHAPTER 3
STRUCTURES AND ANTIMICROBIAL ACTIVITY OF METABOLITES FROM *FUSARIUM* SP.

3.1 Introduction

Naphthoquinones and related metabolites are widely distributed in nature and have been found in higher plants, fungi and actinomycetes. This class of compounds has attracted interest due to their broad-range biological action: phytotoxic, insecticidal, antibacterial and fungicidal.[1, 2)]

The fungus *Fusarium* is a well known soil-borne saprophytic and parasitic fungus that produces diverse bioactive secondary metabolites; for example, fumonisins, trichothecenes and zearalenone are mycotoxins,[3)] fusaric acid and moniliformin are phytotoxins,[4)] and gibberellins are phytohormones.[5)] A number of *Fusarium* fungi also produce naphthoquinones and related metabolites as fungal pigments; they include javanicin, fusarubin, anhydrofusarubin, 4a,10a-dihydrofusarubin, marticin and others.[6)] Among them, 4a,10a-dihydrofusarubins A and B were isolated first in 1978 from *F. solani* as true metabolites before non-enzymatically oxidation to give fusarubin,[7)] and later 3-*O*-ethyl ether of 4a,10a-dihydrofusarubins A was isolated from *F. solani* [8,9)] and 3-*O*-methyl ether of 4a,10a-dihydrofusarubins A together with 3-*O*-ethyl ether was isolated from *F. martii*.[10)]

The biosynthetic origin of 4a,10a-dihydrofusarubins was proposed to be a single-chain heptaketide based on incorporation experiments using ^{13}C-labeled acetate.[11)] Unique 10a-hydroxy-4a,10a-dihydrofusarubins were isolated as antibiotic

pigments from *F. solani*,[12,13] but their structures were revised to those of 4a,10a-dihydrofusarubins.[8] In 2011, 5-hydroxy-4a,10a-dihydrofusarubins were isolated from *Fusarium* sp. BCC14842, and some of them were shown to have antimycobacterial and cytotoxic activities.[14]

Here I describe the isolation and structure elucidation of anhydrofusarubin and five new 3-*O*-alkyl-4a,10a-dihydrofusarubins produced by *Fusarium* sp. Mj-2, and also their antimicrobial activity, together with the antimicrobial activity of 3-*O*-methyl-4a,10a-dihydrofusarubin A synthesized.

3.2 Isolation and structure determination of compounds 11-16

The fungus, strain Mj-2, was isolated from a soil sample collected in Reisekizan of Tottori Prefecture, Japan and classified into the genus *Fusarium* according to the morphological features of its hyphae and conidia, and the sequence of the segment (accession number AB753840) in its 18S rRNA. The Mj-2 was cultured on a malt extract medium without shaking at 24˚C for 14 days in the dark. The metabolites in the culture filtrate were extracted with EtOAc. The extract was purified by chromatographic separations to give compounds **11**–**16** in respective yields of 1.2, 0.3, 0.2, 0.1, 0.7 and 0.1 mg/L.

Compound **11** was obtained as a purple solid. The molecular formula of $C_{15}H_{12}O_6$ was determined by its HR-ESI-TOFMS and NMR data. The spectroscopic data (NMR, UV) agreed well with the reported data for anhydrofusarubin.[9, 11] The structure of compound **11** is shown in Fig 3-1.

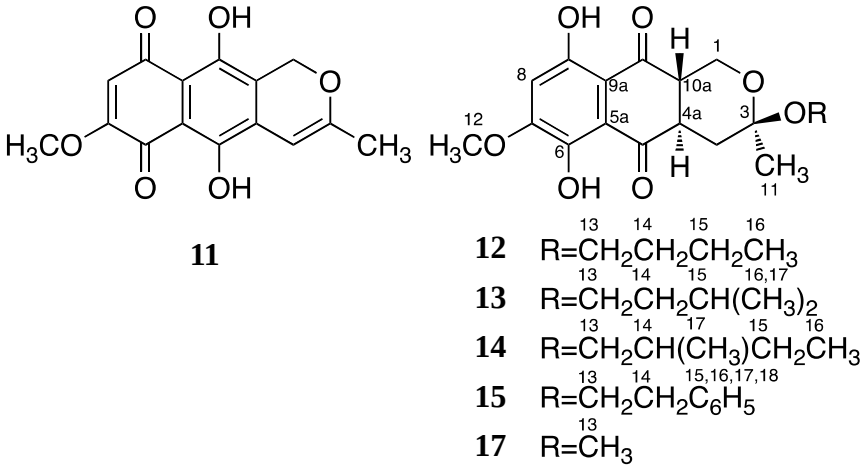

Fig. 3-1. Structures of compounds **11**-**15** and **17**.

Compound **12** was obtained as yellow oil. The molecular formula was established as $C_{19}H_{24}O_7$ (eight unsaturations) on the basis of the HR-ESI-TOFMS and NMR data (Tables 3-1 and 3-2). The ^{13}C NMR spectrum of compound **12** showed the presence of three methyls (one methoxyl), five methylenes (two oxygenated), three methines (two sp^3 and one sp^2), and eight quaternary (two carbonyl, three oxygenated sp^2 and one ketal) carbons. The structural units (a) and (b) in compound **12** (Fig. 3-2) were established as follows.

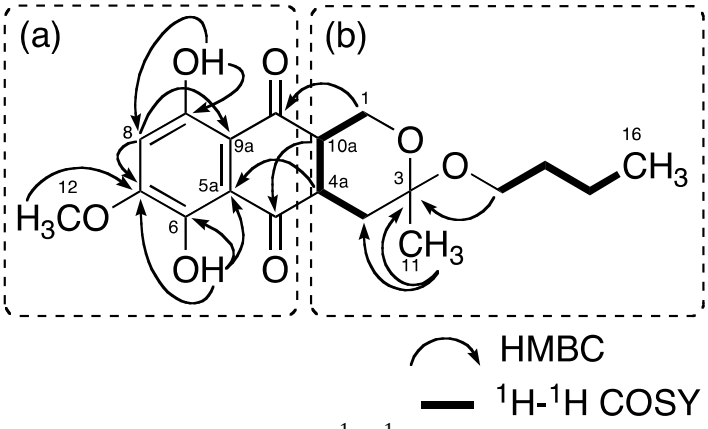

Fig. 3-2. Key HMBC and ^1H-^1H COSY correlations in compound **12**.

Table 3-1. ^{1}H (600 MHz) NMR data for compounds **12-17** in $CDCl_3$.

Position	**12** δ_H (mult., *J* in Hz)	**13** δ_H (mult., *J* in Hz)	**14** δ_H (mult., *J* in Hz)	**15** δ_H (mult., *J* in Hz)	**16** δ_H (mult., *J* in Hz)	**17** δ_H (mult., *J* in Hz)
1	4.20 (dd, 11.6, 4.7)	4.21 (dd, 11.4, 4.7)	4.20 (dd, 11.6, 4.8)	3.98 (dd, 11.6, 4.8)	4.31 (dd, 11.7, 1.2)	4.21 (dd, 11.6, 4.7)
	3.83 (dd, 11.6, 10.8)	3.82 (dd, 11.4, 10.7)	3.84 (dd, 11.6, 10.8)	3.27 (dd, 11.6, 10.8)	3.09 (dd, 11.7, 3.3)	3.82 (dd, 11.6, 10.8)
4	2.42 (dd, 13.5, 3.7)	2.41 (dd, 13.5, 3.6)	2.43 (dd, 13.6, 3.7)	2.39 (dd, 13.5, 3.5)	1.99 (ddd, 13.0, 4.5, 0.9)	2.40 (dd, 13.8, 3.8)
	1.66 (dd, 13.5, 11.6)	1.67 (dd, 13.5, 11.6)	1.66 (dd, 13.6, 11.6)	1.60 (dd, 13.5, 11.6)	1.54 (t, 13.0)	1.69 (dd, 13.8, 11.6)
4a	3.43	3.43	3.42	3.27	3.49	3.41
	(ddd, 13.1, 11.6, 3.7)	(ddd, 13.2, 11.6, 3.6)	(ddd, 13.2, 11.6, 3.7)	(ddd, 13.0, 11.6, 3.5)	(ddd, 13.0, 5.4, 4.5)	(ddd, 13.2, 11.6, 3.8)
6-OH	12.07 (s) 12.07 (s)	12.08 (s)	12.03 (s)	12.39 (s)	12.05 (s)	
8	6.66 (s) 6.66 (s)	6.67 (s)	6.67 (s)	6.69 (s)	6.66 (s)	
9-OH	12.21 (s) 12.22 (s)	12.22 (s)	12.23 (s)	12.66 (s)	12.20 (s)	
10a	2.95	2.95	2.95	2.83	2.71 (m)	2.95
	(ddd, 13.1, 10.8, 4.7)	(ddd, 13.2, 10.7, 4.7)	(ddd, 13.2, 10.8, 4.8)	(ddd, 13.0, 10.8, 4.8)		(ddd, 13.2, 10.8, 4.7)
11	1.42 (s)	1.43 (s)	1.42 (s)	1.39 (s)	1.26 (s)	1.41 (s)
12	3.96 (s)	3.96 (s)	3.96 (s)	3.97 (s)	3.96 (s)	3.96 (s)
13	3.44 (t, 6.8)	3.46 (br.t, 7.2)	3.31 (dd, 9.0, 6.2)	3.67 (ddd, 9.2, 6.8, 5.8)	3.69 (ddd, 9.0, 6.4, 6.4)	3.23 (s)
			3.21 (dd, 9.0, 6.8)	3.62 (ddd, 9.2, 8.0, 6.9)	3.62 (ddd, 9.0, 7.6, 6.9)	
14	1.52 (tt, 7.4, 6.8)	1.42 (m)	1.59 (m)	2.84 (m)	2.90 (m)	
15	1.36 (sex, 7.4)	1.66 (m)	1.43 (m)			
			1.13 (m)			
16	0.91 (t, 7.4)	0.90 (d, 6.5)	0.88 (t, 7.5)	7.23-7.18 (m)	7.32-7.27 (m)	
17		0.89 (d, 6.5)	0.89 (d, 6.9)	7.23-7.18 (m)	7.32-7.27 (m)	
18				7.15 (m)	7.20 (m)	

The ^{1}H and ^{13}C NMR data revealed the presence of two chelated hydroxy protons (δ_H 12.07 and 12.21) and penta-substituted benzene (δ_H 6.66, δ_C 106.4, 107.3, 114.1, 146.1, 156.8 and 157.7). The aromatic proton (δ_H 6.66, 8-H) was linked to the carbon (δ_C 106.4, C-8) of the benzene moiety on the basis of HMQC data. The HMBC data

Table 3-2. ^{13}C (150 MHz, δ in ppm) NMR data for compounds **12**-**17** in $CDCl_3$.

Position	**12**	**13**	**14**	**15**	**16**	**17**
1	59.5	59.5	59.5	59.2	56.0	59.5
3	97.5	97.5	97.4	97.5	96.4	97.7
4	35.4	35.3	35.4	35.1	37.8	35.0
4a	43.4	43.3	43.4	43.1	43.1	43.2
5	198.8	198.8	198.8	198.5	198.7	198.7
5a	114.1	114.1	114.1	114.1	112.6	114.0
6	146.1	146.1	146.1	145.9	147.0	146.1
7	156.8	156.8	156.8	156.7	156.9	156.8
8	106.4	106.4	106.4	106.4	106.8	106.4
9	157.7	157.7	157.7	157.7	157.9	157.7
9a	107.3	107.3	107.3	107.2	107.0	107.3
10	203.0	203.0	203.0	203.0	204.7	202.8
10a	45.9	45.9	45.9	45.5	43.4	45.8
11	24.0	24.0	24.0	23.9	24.0	23.2
12	56.6	56.6	56.6	56.6	56.6	56.6
13	60.1	58.8	65.4	61.4	61.7	48.0
14	32.0	38.7	35.1	36.4	36.4	
15	19.6	25.2	26.4	139.3	139.5	
16	14.0	22.8	11.3	129.1[a]	129.2[b]	
17		22.6	16.8	128.2[a]	128.3[b]	
18				126.4	126.3	

[a,b] interchangeable within the same sign

revealed that the methoxyl group (δ_H 3.96, C-12) and the two chelated hydroxyls (δ_H 12.07 and 12.21) were bound to C-7, C-6 and C-9 of the benzene moiety, respectively. The HMBC correlations of 8-H to C-7 and C-9a, of 6-OH to C-5a and C-7, and of 9-OH to C-8 established the substitution pattern of the benzene ring. Two ketonic carbonyl carbons chelated to the two phenolic hydroxyls were connected to the benzene ring to afford the structural unit (a) shown in Fig. 3-2. The structural unit (b) was also established by 1D and 2D NMR data. ^{1}H-^{1}H COSY and HMQC data indicated two coupling systems, a butoxy group (δ_H 0.91, 1.36, 1.52 and 3.44, δ_C 14.0, 19.6, 32.0 and 60.1) and -O-C(1)H_2-C(10a)H-C(4a)H-C(4)H_2- (δ_H 4.20, 3.83, 2.95, 3.43, 2.42 and 1.66, δ_C 59.5, 45.9, 43.4 and 35.4). The HMBC correlations of methyl protons (δ_H 1.42, 11-H) to the ketal carbon (δ_C 97.5, C-3) and C-4 (δ_C 35.4) indicated the connection of the ketal carbon (C-3) to the methyl (C-11) and methylene (C-4) carbons, and the HMBC correlation of 13-H (δ_H 3.44) of the butoxy group to the ketal carbon (C-3) indicated the connection of the butoxy group to C-3. Considering the number of oxygen atoms in the molecule, C-3 must be connected to C-1 through oxygen to give structural unit (b) containing tetrahydropyran moiety. There were two ways to connect structural unit (a) to structural unit (b). The HMBC correlations of 1-H to the ketone carbon (C-10), of 10a-H to the another ketone carbon (C-5) and of 4a-H to C-5a of the benzene ring determined the connection between the structural units (a) and (b) exclusively. As shown in Fig. 3-1, the structure of compound **12** thus established has never been reported, but it closely relates to 4a,10a-dihydrofusarubin A and its *O*-methyl and *O*-ethyl ethers reported by Kurobane *et al.*[7, 10] The ring portion of compound **12** is the same as that of 4a,10a-dihydrofusarubin A and its *O*-methyl and *O*-ethyl ethers, and

their NMR data of the ring portion were almost the same.

The relative stereochemistry of compound **12** was determined based on ^{1}H-^{1}H coupling constants and NOESY correlations. The large coupling constants ($J_{1\text{-H}\alpha\ 10a\text{-H}}$ = 10.8 Hz, $J_{10a\text{-H},\ 4a\text{-H}}$ = 13.1 Hz and $J_{4a\text{-H},\ 4\text{-H}\beta}$ = 11.6 Hz) indicated that the tetrahydropyran ring had a chair form and these protons occupied axial positions, being similar to those of 3-*O*-methyl and 3-*O*-ethyl-4a,10a-dihydrofusarubin A.[10] The NOESY spectrum of compound **12** showed the NOE correlations of 3-methyl protons to 4-Hα, 4a-H and 1-Hα. This indicated that the methyl, 4a-H and 1-Hα were mutually in 1,3-diaxial relations on a chair form of the tetrahydropyran ring as shown in Fig. 3-3. On the basis of these data, the stereochemistry of compound **12** was determined to be 3*R**, 4a*R**, l0a*S**. It was notable that the stereochemistry of 3-*O*-methyl and 3-*O*-ethyl-4a,10a-dihydrofusarubin A was reported to be 3*S**, 4a*R**, l0a*S** [10] and different from that of compound **12**. However, the previous authors[10] provided no spectroscopic evidence that indicates the stereochemistry at C-3 of these compounds. To verify the stereochemistry of 3-*O*-methyl-4a,10a-dihydrofusarubin A, compound **12** was reacted with MeOH in the presence of *p*-toluenesulfonic acid to afford compound **17**.

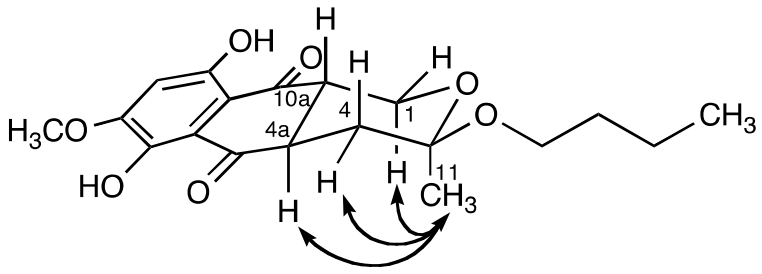

Fig. 3-3. Key NOESY correlations in compound **12**.

The ^{1}H and ^{13}C NMR data, including the coupling constants between 1-Hα and 10a-H (10.8 Hz), between 10a-H and 4a-H (13.2 Hz), and between 4a-H and 4-Hβ (11.6 Hz) and the optical rotation well agreed with those reported for 3-*O*-methyl-4a,10a-dihydrofusarubin A.[10] The NOESY spectrum of our derivative showed the same NOE correlations as those of compound **12**; NOE correlations of 3-methyl protons to 4-Hα, 4a-H and 1-Hα, were detected and no NOE correlations of 3-*O*-methyl protons to these protons were observed. These findings indicated that the stereochemistry of 3-*O*-methyl-4a,10a-methyldihydrofusarubin A was 3*R**, 4a*R**, l0a*S**, which was the same as that of compound **12**, and thus the stereochemistry reported for 3-*O*-methyl and 3-*O*-ethyl-4a,10a-dihydrofusarubin A should be corrected.

Compound **13** was isolated as a light orange solid, and the molecular formula was established as $C_{20}H_{26}O_7$ from the HR-ESI-TOFMS and NMR data. A detailed analysis of the NMR data (Tables 3-1 and 3-2), in particular the ^{1}H-^{1}H COSY, HMQC and HMBC spectra, revealed that the ring portion (C1 to C12) of compound **13** was the same as that of compound **12**, but that *O*-alkyl at C-3 was different. On the bases of the ^{1}H-^{1}H COSY and HMBC correlations, the *O*-alkyl in compound **13** was found to be 3-methylbutoxy in place of butoxy in compound **12**. The key NOE correlations were identical to those of compound **12**, indicating that compounds **12** and **13** possessed the same relative stereochemistry. The structure of compound **13** was confirmed by the conversion of compound **12** into compound **13** with 3-methyl-1-butanol under conditions similar to those used for the preparation of 3-*O*-methyl-4a,10a-dihydrofusarubin A.

Compound **14** was isolated as a light orange solid, and the molecular formula was

established as $C_{20}H_{26}O_7$ from the HR-ESI-TOFMS and NMR data. A detailed analysis of the NMR data revealed the structure. The key NOE correlations indicated that compounds **12** and **14** possessed the same relative stereochemistry in the ring. The stereochemistry of *O*-alkyl in compound **14** was determined as follows. Treating compound **12** with (±)-2-methyl-1-butanol under conditions similar to those used for the preparation of 3-*O*-methyl-4a,10a-dihydrofusarubin A gave the mixture of compound **14** and its diastereomer. They were separable on the chiral HPLC and showed the similar UV absorption pattern and MS profiles; compound **14** was eluted at 9.7 min and its diastereomer at 10.1 min. The product synthesized with compound **12** and *S*-(–)-2-methyl-1-butanol was eluted at 9.7 min, indicating that the absolute configuration of C-14 is *S*.

Compound **15** was isolated as a light orange solid, and the molecular formula was established as $C_{23}H_{24}O_7$ from the HR-ESI-TOFMS and NMR data. Compound **15** has the same tricyclic unit of compounds **12**–**14** on the basis of its NMR data, but the 3-*O*-alkyl portion of compound **15** was 2-phenylethoxy (Tables 3-1 and 3-2). The key NOE correlations indicated that compounds **12**–**14** and **15** possessed the same relative stereochemistry. The structure of compound **15** was also confirmed by the conversion of compound **12** into compound **15** with 2-phenylethanol under the conditions mentioned above.

Compound **16** was isolated as a light orange solid. The molecular formula was established as $C_{23}H_{24}O_7$ from the HR-ESI-TOFMS and NMR data and the same as that of **15**. The 2D NMR data revealed that compounds **15** and **16** have the same structure without considering the stereochemistry. Although the ^{1}H NMR spectrum of compound

16 was very similar to that of compound **15,** the resonances of some protons on the tetrahydropyran ring of compounds **16** and **15** were different in their chemical shifts [δ_H 4.31, 3.09 (1-H), 2.71 (10a-H), 3.49 (4a-H), and 1.99, 1.54 (4-H) for **16**; δ_H 3.98, 3.27 (1-H), 2.83 (10a-H), 3.27 (4a-H), and 2.39, 1.60 (4-H) for **15**] and shapes ($J_{4a\text{-}H,10a\text{-}H}$ = 5.4 Hz for **16**; $J_{4a\text{-}H,10a\text{-}H}$ = 13.0 Hz for **15**) as shown in Table 3-1. Since these differences in ^{1}H NMR data between compounds **15** and **16** were almost the same between 4a,10a-dihydrofusarubin A and its diastereomer 4a,10a-dihydrofusarubin B,[7] the relative stereochemistry of compound **16** was suggested to be 3*R**, 4a*R**, 10a*R**. However, the reported stereochemistry of 4a,10a-dihydrofusarubin B was not definitive because of the lack of its NOE data. In addition, I could not measure the NOESY of compound **16** because of a shortage of the sample. Therefore, further studies are needed to establish its stereochemistry definitively.

3.3 Antimicrobial activities of compounds 11-17

The antifungal and antibacterial activity of compounds **11**–**17** against the fungi, *Magnaporthe grisea*, *Aspergillus oryzae* and *Penicillium citrinum*, and the Gram-positive bacteria *Bacillus subtilis* and *Staphylococcus aureus*, and Gram-negative bacteria *Escherichia coli* and *Pseudomonas aeruginosa*, was evaluated (Table 3-3). Among the compounds, compound **11** exhibited the most potent, but moderate to weak activity against the fungi, *P. citrinum* (MIC 100 μg/mL), *M. grisea* (MIC 300 μg/mL) and *A. oryzae* (MIC 1000 μg/mL), and the bacteria, *B. subtilis*, *S. aureus* and *E. coli* (MIC 100 μg/mL) and *P. aeruginosa* (MIC 1000 μg/mL). Compound **17** also exhibited moderate to weak antifungal activities against *P. citrinum* (MIC 100 μg/mL), *M. grisea*

(MIC 300 μg/mL) and *A. oryzae* (MIC 1000 μg/mL), and weak antibacterial activity against *S. aureus* (MIC 300 μg/mL) and *P. aeruginosa* (MIC 1000 μg/mL). Compound **12** exhibited weak antifungal activities against *P. citrinum* (MIC 300 μg/mL) and *M. grisea* (MIC 1000 μg/mL) and weak antibacterial activities against *S. aureus* (MIC 300 μg/mL) and *P. aeruginosa* (MIC 1000 μg/mL). Below 1000 μg/mL, compounds **13**–**16** did not show any antifungal activity against three fungi tested and any antibacterial activity against *B. subtilis*, *E. coli*, and *P. aeruginosa*, while compounds **13** and **14** showed weak antibacterial activity only against *S. aureus* (MIC 1000 μg/mL). The results indicate that the size of the *O*-alkyl portion negatively affects the antimicrobial activity, and that 4a,10a-dihydrofusarubin A would exhibit stronger antimicrobial activity than any of 3-*O*-alkyl-4a,10a-dihydrofusarubins if it was tested.

Table 3-3. Antimicrobial activities of compounds **11-17**.

Compound	Antifungal, MIC (μg/mL)			Antibacterial, MIC (μg/mL)			
	M. grisea	*A. oryzae*	*P. citrinum*	*B. subtilis*	*S. aureus*	*E. coli*	*P. aeruginosa*
11	300	1000	100	100	100	100	1000
12	1000	>3000	300	>1000	300	>1000	1000
13	>3000	>3000	>3000	>1000	1000	>1000	>1000
14	>3000	>3000	>3000	>1000	1000	>1000	>1000
15	>3000	>3000	>3000	>1000	>1000	>1000	>1000
16	>3000	>3000	>3000	>1000	N.T.[a]	>1000	>1000
17	300	1000	100	>1000	300	>1000	1000

[a] not tested

3.4 Experiments

3.4.1 General experimental procedures

NMR spectra were measured with a Bruker Biospin Avance II 600 MHz spectrometer. Chemical shifts were referenced to $CDCl_3$ (δ_H 7.26, δ_C 77.0). ESI-TOFMS and HR-ESI-TOFMS spectra were obtained with a Waters LCT Premier XE mass spectrometer. Optical rotations were measured with a Horiba SEPA-500 polarimeter. UV and visible spectra were recorded with a Hitachi U-2001 spectrophotometer. A Shimadzu LC-6A chromatograph system was used for analytical and preparative HPLC.

3.4.2 Fungal materials

The fungal strain Mj-2 was first isolated from a soil sample at Reisekizan, Tottori Prefecture, Japan, and classified as *Fusarium* sp., based on its morphological features. PCR was carried out using ITS2 and ITS5 as primers and its genomic DNA as a template and the PCR product was sequenced using ITS2 as a primer. Its sequence (223 bases, Accession number AB753840) was found to be very similar (99%) to that of *Fusarium solani* by blast search. The fungus was maintained on potato dextrose agar slants.

3.4.3 Fermentation and isolation

The fungus was grown without shaking at 25°C for 14 days in the dark in 500-mL conical flasks (50) containing a liquid medium (200 mL/flask) composed of glucose (30 g/L), peptone (3 g/L), the extract from 50 g/L of malt, and tap water. Metabolites were extracted from the culture filtrate with EtOAc (10 L x 3) after adjusting the pH to 2.0

with 6 M HCl. The EtOAc solution was dried over Na_2SO_4, and evaporated to dryness to give a residue (1.92 g). This residue was subjected to Si gel CC (4.8 x 150 mm, Daiso gel IR-60, Daiso, Co., Ltd., Osaka, Japan), with 2000 mL (400 mL x 5) each of 5%, 10%, 20% and 30% (v/v) acetone in *n*-hexane as the eluent. The third fraction (19.2 mg) eluted with 5% (v/v) acetone in *n*-hexane, was purified by HPLC using a COSMOSIL $5C_{18}$-AR-II column (10 x 250 mm, NACALAI TESQUE, INC., Kyoto, Japan) and, MeOH-H_2O (9:1, v/v) as the mobile phase at a flow rate of 1.0 mL/min, with monitoring at 220, 250 and 280 nm to afford compounds **11** (11.7 mg) and **12** (2.7 mg). The retention times of compounds **11** and **12** were 43.0 and 55.6 min, respectively. The first fraction (12.0 mg) eluted with 10% (v/v) acetone in *n*-hexane, was purified by HPLC using a COSMOSIL $5C_{18}$-AR-II column (10 x 250 mm), eluted with MeCN-H_2O (7:3, v/v) at a flow rate of 2.0 mL/min, with monitoring at 220, 280 and 340 nm to afford compounds **13** (2.1 mg) and **14** (1.2 mg). The retention times of compounds **13** and **14** were 26.3 and 28.1 min, respectively. The second fraction (23.4 mg) eluted with 10% (v/v) acetone in *n*-hexane, was purified by HPLC using a COSMOSIL $5C_{18}$-AR-II column (10 x 250 mm), eluted with MeOH-H_2O (13:7, v/v) at a flow rate of 2.2 mL/min, with monitoring at 220, 280 and 340 nm to afford compounds **15** (6.9 mg) and **16** (0.9 mg). The retention times of compounds **15** and **16** were 28.8 and 30.5 min, respectively.

Compound **11**. Purple solid. $[\alpha]^{24}_{D}$ +235° (*c* 0.64, acetone). UV and visible λ_{max} (MeOH) nm (ε): 202 (11,900), 231 (10,900), 287 (9300), 535 (4800). HR-ESI-TOFMS *m/z* ($[M+H]^+$): Calcd. for $C_{15}H_{13}O_6$: 289.0712, Found: 289.0711. NMR δ_H 13.03 (1H, s, OH), 12.64 (1H, s, OH), 6.16 (1H, s, 8-H), 5.98 (1H, s, 4-H), 5.21 (2H, s, 1–H), 3.92 (3H, s, 7-OMe), 2.01 (3H, s, 3-Me); δ_C 182.9, 177.9, 161.5, 160.0, 157.9, 157.8, 133.1, 122.7, 110.9, 110.0, 108.0, 94.7, 63.0, 56.7, 20.1.

Compound **12**. Yellow oil. $[\alpha]^{24}_{D}$ +146° (*c* 0.36, acetone). UV and visible λ_{max} (MeOH) nm (ε): 224 (8500), 301 (2400), 392 (1000), 495 (1700). HR-ESI-TOFMS *m/z* ($[M+H]^+$): Calcd. for $C_{19}H_{25}O_7$: 365.1600, Found: 365.1602. NMR data: see Tables 3-1 and 3-2.

Compound **13**. Light orange solid. $[\alpha]^{24}_{D}$ +154° (*c* 0.24, acetone). UV and visible λ_{max} (MeOH) nm (ε): 224 (8400), 302 (2200), 495 (1900). HR-ESI-TOFMS *m/z* ($[M+H]^+$): Calcd. for $C_{20}H_{27}O_7$: 379.1757, Found: 379.1762. NMR data: see Tables 3-1 and 3-2.

Compound **14**. Light orange solid. $[\alpha]^{24}_{D}$ +143° (*c* 0.12, acetone). UV and visible λ_{max} (MeOH) nm (ε): 224 (9500), 303 (2500), 495 (1900). HR-ESI-TOFMS *m/z* ($[M+H]^+$): Calcd. for $C_{20}H_{27}O_7$: 379.1757, Found: 379.1751. NMR data: see Tables 3-1 and 3-2.

Compound **15**. Light orange solid. $[\alpha]^{24}_{D}$ +146° (*c* 0.46, Acetone). UV and visible λ_{max} (MeOH) nm (ε): 209 (8800), 241 (7800), 273 (2900), 300 (2300), 389 (3700), 496 (400). HR-ESI-TOFMS *m/z* ($[M+H]^+$): Calcd. for $C_{23}H_{25}O_7$: 413.1600, Found: 413.1598. NMR data: see Tables 3-1 and 3-2.

Compound **16**. Light orange solid. $[\alpha]^{24}_{D}$ +12° (*c* 0.40, acetone). UV and visible λ_{max} (MeOH) nm (ε): 208 (8900), 242 (7400), 274 (2700), 301 (2200), 391 (3300), 496 (500). HR-ESI-TOFMS *m/z* ($[M+H]^+$): Calcd. for $C_{23}H_{25}O_7$: 413.1600, Found: 413.1610. NMR data: see Tables 3-1 and 3-2.

3.4.4 Conversion of compound 12 into compounds 13, 14, 15 and 17

Several mg of compound **12** were dissolved in acetone (500 μL), to which the reagent (500 μL, 3-methylbuthanol for compound **13**, (*S*)-(−)-2-methyl-1-butanol for

compound **14**, 2-phenylethanol for compound **15**, MeOH for compound **17**, Wako Pure Chemical Industries, Ltd., Osaka, Japan) and a small amount of *p*-toluenesulfonic acid monohydrate (Wako Pure Chemical Industries, Ltd.) were added. The mixture was stirred vigorously at 0°C for 30 min under N_2. The reaction mixture was poured into brine (3 mL) and extracted with EtOAc (3 mL x 3), and the combined organic layer was washed with 1M NH_4Cl (10 mL). The EtOAc solution was dried over Na_2SO_4 and evaporated under a vacuum to dryness to give each compound; the yield was 4.1 mg of compound **13**, 3.4 mg of compound **14**, 4.2 mg of compound **15**, and 2.0 mg of compound **17** from 4.7, 4.2, 5.1 and 2.7 mg of compound **2**, respectively. To determine the stereochemistry of *O*-alkyl of compound **14**, 1.6 mg of compound **12** was treated with (±)-2-methyl-1-butanol according to the method described above. The product was purified by HPLC using a COSMOSIL 5C_{18}-AR-II column (10 x 250 mm) and, MeOH-H_2O (7:3, v/v) as the mobile phase at a flow rate of 2.5 mL/min to afford the mixture of compound **14** and its diastereomer. The retention time of the mixture was around 22 min. The mixture was then analyzed by chiral HPLC using a CHIRALCEL OD column (4.6 x 250 mm, DAICEL Corporation, Osaka, Japan) and, *n*-hexane-EtOH (7:3, v/v) as the mobile phase at a flow rate of 0.8 mL/min, with monitoring at 220, 254, 280 and 320 nm. The retention times of compound **14** and its diastereomer were 9.7 and 10.1 min, respectively. The eluates from the chiral HPLC column were collected and analyzed with a Waters LCT Premier XE mass spectrometer.

Compound **17**. Purple solid. $[\alpha]^{24}_{D}$ +122° (*c* 0.46, acetone). ESI-TOFMS *m/z* 323.1 ($[M+H]^+$). NMR data: see Tables 3-1 and 3-2.

3.4.5 Antifungal assay

Each compound was dissolved in MeOH (10 μL), and placed into wells of a 96-microwell plate. As a control, MeOH was also placed in the plate. After air-drying, 100 μL of GY medium composed of 2% glucose, 0.5% yeast extract, and 1.5% agar was added to the wells. The fungal spores (8 x 10^3 spores/mL) were inoculated onto the medium. *Magnaporthe grisea* (*Pyricularia oryzae* IFO 30733), *Aspergillus oryzae* AEM 42 and *Penicillium citrinum* ATCC 9849 were used. After incubation for 3 days at 28°C, the mycelium growth was observed and the minimum concentration to inhibit the growth of mycelia was determined. This assay was carried out four times.

3.4.6 Antibacterial assay

The MeOH solutions of the compounds were placed into wells of a 96-microwell plate. As a control, MeOH was also placed in the plate. After air-drying, 100 μL of LB medium composed of 0.5% yeast extract, 1% tryptone, 1% NaCl and 1% agar was added to the wells. Then, 10 μL of the bacterium suspension in the same LB medium (10^4-10^5 cells/mL) was inoculated onto the medium. *Bacillus subtilis* AEM 162, *Staphylococcus aureus* NBRC 100910, *Escherichia coli* IFO 3301, and *Pseudomonas aeruginosa* NBRC 106052 were used. After incubation for one day at 28°C, the growth was observed and the minimum concentration to inhibit the growth of the bacteria was determined. This assay was carried out four times.

3.5 References

1. Medentsev AG, Akimenko VK, 1998, Naphthoquinone metabolites of the fungi, *Phytochemistry*, **47**, 935-959.
2. Bebula P, Adam V, Havel L, Kizek R, 2009, Noteworthy secondary metabolites

naphthoquinones - their occurrence, pharmacological properties and analysis, *Curr. Pharm. Anal.*, **5**, 47-68.

3. Yazar S, Omurtag GZ, 2008, Trichothecenes and zearalenone in cereals, *Int. J. Mol. Sci.*, **9**, 2062-2090.
4. Abbas HK, Boyette CD, Hoagland RE, 1995, Phytotoxicity of *Fusarium*, other fungal isolates, and of the phytotoxins fumonisin, fusaric acid, and moniliformin to jimsonweed, *Phytoprotection*, **76**, 17-25.
5. Bhalla K, Singh SB, Agarwal, R, 2010, Quantitative determination of gibberellins by high performance liquid chromatography from various gibberellins producing *Fusarium* strains, *Environ. Monit. Assess.*, **167**, 515-520.
6. Cole RJ, Schweikert MA, 2003, "Handbook of secondary fungal metabolites, volume I," Academic Press, San Diego, pp. 837-896.
7. Kurobane I, Vining LC, McInnes AG, Smith DG, 1978, Diastereoisomeric 4a,10a-dihydrofusarubins: True metabolites of *Fusarium solani1*, *Can. J. Chem.*, **56**, 1593-1594.
8. Kurobane I, Vining LC, McInnes AG, Gerber NN, 1980, Metabolites of *Fusarium solani* related to dihydrofusarubin, *J. Antibiot.*, **33**, 1376-1379.
9. Tatum JH, Baker RA, 1983, Naphthoquinones produced by *Fusarium solani* isolated from citrus, *Phytochemistry*, 22, 543-547.
10. Kurobane I, Zaita N, Fukuda A, 1986, New Metabolites of *Fusarium martii* related to dihydrofusarubin, *J. Antibiot.*, **39**, 205-214.
11. Kurobane I, Vining LC, McInnes AG, Walter JA, 1980, Use of ^{13}C in biosynthetic studies. The labeling pattern in dihydrofusarubin enriched from [^{13}C]- and [^{13}C, ^{2}H]acetate in cultures of *Fusarium solani*, *Can. J. Chem.*, **58**, 1380-1385.

12. Ammar MS, Gerber NN, McDaniel LE, 1979, New antibiotic pigments related to fusarubin from *Fusarium solani* (Mart.) Sacc. I. Fermentation, isolation, and antimicrobial activities, *J. Antibiot.*, **32**, 679-684.
13. Gerber NN, Ammar MS, 1979, New antibiotic pigments related to fusarubin from *Fusarium solani* (Mart.) Sacc. II. Structure elucidations, *J. Antibiot.*, **32**, 685-688.
14. Kornsakulkarn J, Dolsophon K, Boonyuen N, Boonruangprapa T, Rachtawee P, Prabpai S, Kongsaeree P, Thongpanchang C, 2011, Dihydronaphthalenones from endophytic fungus *Fusarium* sp. BCC14842, *Tetrahedron*, **67**, 7540-7547.
15. Shao CL, Wang CY, Deng DS, She ZG, Gu YC, Lin YC, 2008, Crystal structure of a marine natural compound, anhydrofusarubin, *Chin. J. Struct. Chem.*, **27**, 824-828.

CHAPTER 4

CONCLUSION

The biosynthetic pathway of phytotoxin radicinin (**3**) was previously proposed on the basis of structural features of radicinin and its analoghs. In the present research, precursor administration and cell-free experiments with deoxyradicinin and radicinin were carried out in *Bipolaris coicis* H13-3, and a new biosynthetic relationship was found. In the new biosynthetic relationship, first, deoxyradicinin (**1**) is converted to radicinin (**3**) catalyzed by deoxyradicinin monooxygenase. Then, radicinin epimerase catalyzes the epimerization of radicinin (**3**) at C-3 to 3-*epi*-radicinin (**4**) reversibly. Finally, 3-*epi*-radicinin (**4**) is probably converted to 3-*epi*-radicinol (**5**) by stereospecific reduction at C-4, followed by epoxidation of the side chain in 3-*epi*-radicinol (**5**). The toxicity of radicinin for tear glass, *Coix lachryma-jobi* L., was ten times higher than that of 3-*epi*-radicinin, and hence it was hypothesized that radicinin epimerase regulates the pathogenicity of the fungus to the plants. Deoxyradicinin monooxygenase and radicinin epimerase were also characterized in this study.

To clarify the function and the role of antimicrobial substances produced by phytopathogenic fungi, a screening of new antimicrobial metabolites from soil-borne saprophytic and parasitic fungi was performed. *Fusarium* sp. (Mj-2) was found to produce five new 3-*O*-alkyl-4a,10a-dihydrofusarubins in the culture filtrate together with a known metabolite, anhydrofusarubin (**11**). The structures of the new metabolites were shown by spectroscopic analyses to be 3-*O*-butyl (**12**), 3-*O*-3’-methylbutyl (**13**), 3-*O*-2’-methylbutyl (**14**) and 3-*O*-2’-phenylethyl-4a,10a- dihydrofusarubin A (**15**), and an isomer of the 3-*O*-2’-phenylethyl-4a,10a-dihydrofusarubin A (**16**). Their antifungal

and antibacterial activities were evaluated together with those of 3-*O*-methyl derivative (**17**) prepared from 3-*O*-butyl-4a,10a-dihydrofusarubin A (**12**), indicating that the size of the *O*-substituent at C-3 in the 4a,10a-dihydrofusarubins negatively affects the metabolites' antimicrobial activity.

ACKNOWLEDGEMENTS

I would like to my deep gratitude, and sincere appreciation to Professor Hiromitsu Nakajima of Tottori University for his encouragement, advice and support. I also wish to express my deep appreciation to Associate Professor Atsushi Ishihara of Tottori University and Professor Yoshihisa Ozoe of Shimane University for their useful advice. I am heartily grateful to Professor Jun-ichi Tamura of Tottori University and Dr. Emi Sakuno of the Tottori Mycological Institute of the Japan Kinoko Research Center Foundation for their technical advice and support. I thank to Mr. Naoto Nishida for his technical support. I am also grateful to Ms. N. Inoue, Mr. S. Matsunaga and Mr. Akiyoshi Maeji for his technical assistance. Finally, I would like to thank the students graduated from and present in our laboratory for their help.

LIST OF PUBLICATIONS

CHAPTER 2

1. Suzuki M, Sakuno E, Ishihara A, Tamura J, Nakajima H, 2012, Conversions of deoxyradicinin to radicinin and of radicinin to 3-*epi*-radicinin in the phytopathogenic fungus *Bipolaris coicis*. *Phytochemistry* **75**, 14–20.

CHAPTER 3

2. Suzuki M, Nishida N, Ishihara A, Nakajima H, 2012, New 3-*O*-alkyl-4a,10a-dihydrofusarubins produced by *Fusarium* sp. Mj-2. *Biosci. Biotech. Biochem*. in press.

Summary

Plant diseases caused by plant pathogens are serious problems in agriculture all over the world. Phytopathogenic fungi produce diverse secondary metabolites that show phytotoxic and/or antimicrobial activity and that play important roles in infection and colonization in plants. To know the infection and colonization mechanism by plant pathogens, it is important and necessary to identify the molecules involved in the pathogenesis.

Radicinin (**3**) is a phytotoxic and antibiotic metabolite produced by some phytopathogenic fungi. Precursor administration and cell-free experiments with deoxyradicinin (**1**) and radicinin (**3**) were carried out in *Bipolaris coicis* H13-3. When deoxyradicinin (**1**) was administered to the fungus, radicinin (**3**) and 3-*epi*-radicinin (**4**) formed. When radicinin (**3**) administered, 3-*epi*-radicinin (**4**) was formed. Their formation was confirmed by cell-free experiments. Deoxyradicinin 3-monooxygenase which catalyzes conversion of deoxyradicinin (**1**) to radicinin (**3**) showed the best activity at 35 ℃ and pH 7.0, and required NAD^+ as co-enzyme. Its molecular weight was determined to be 130–184 kDa. Radicinin epimerase catalyzing the reaction of radicinin (**3**) to 3-epi-radicinin (**4**) was purified from a cell-free extract. Radicinin epimerase is a homodimer of a 28 kDa subunit, and its highest activity was achieved at 30–35 ℃ and pH 7.0–9.0. From these results, biosynthesis and metabolism of radicinin was deduced as shown in Fig. 1.

The fungus *Fusarium* is a well known soil-borne saprophytic and parasitic fungus that produces diverse bioactive secondary metabolites. Five new 3-*O*-alkyl-4a,10a-dihydrofusarubins (**12-16**) were isolated from the culture filtrate of a

strain of *Fusarium* sp. (Mj-2) together with a known metabolite, anhydrofusarubin (**11**). The structures of the new metabolites were elucidated by spectroscopic analyses to be 3-*O*-butyl (**12**), 3-*O*-3'-methylbutyl (**13**), 3-*O*-2'-methylbutyl (**14**) and 3-*O*-2'-phenylethyl-4a,10a-dihydrofusarubin A (**15**), and an isomer of the 3-*O*-2'-phenylethyl-4a,10a-dihydrofusarubin A (**16**) (Fig. 2). Their antifungal and antibacterial activities were evaluated together with 3-*O*-methyl derivative (**17**) prepared from 3-*O*-butyl-4a,10a-dihydrofusarubin A (**12**), indicating that the size of the *O*-substituent at C-3 in the 4a,10a-dihydrofusarubins negatively affects the metabolites' antimicrobial activity.

The present study provided insight into the function and role of the secondary metabolites produced by the phytopathogenic fungi in the pathogenesis.

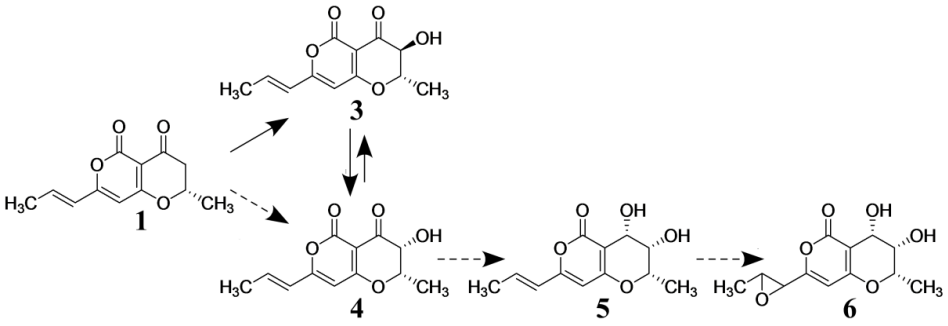

Fig. 1. Biosynthesis and metabolism of radicinin in *Bipolaris coicis* H13-3

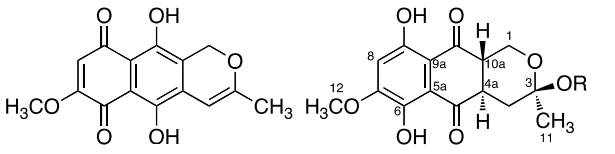

11

12 R=$CH_2CH_2CH_2CH_3$

13 R=$CH_2CH_2CH(CH_3)_2$

14 R=$CH_2CH(CH_3)CH_2CH_3$

15 R=$CH_2CH_2C_6H_5$

17 R=CH_3

Fig. 2. Structures of compounds **11-15** and **17** from *Fusarium* sp. Mj-2

摘要

植物病原菌による作物への被害は、世界中の農業において深刻な問題である。植物病原性糸状菌は、植物毒素や抗生物質などの多様な二次代謝産物を生産しており、それらの化合物は、植物病の発生に大きな役割を果たすことが知られている。 植物病原菌の感染やコロニー形成の分子メカニズムを知るため、病原にかかわる化合物の同定を行うことは非常に重要かつ必要な事項である。

Radicinin (**3**)は植物病原性糸状菌によって生産される植物毒素、抗生物質である。予想される radicinin の生合成前駆体、deoxyradicinin (**1**)や radicinin (**3**)そのものの *Bipolaris coicis* H13-3 株への投与実験、および無細胞系実験を行った。Deoxyradicinin (**1**)を菌体へ投与した際には、radicinin (**3**) と 3-*epi*-radicinin (**4**)が生成され、また radicinin (**3**)を投与した時には、3-*epi*-radicinin (**4**)が生成されることがわかった。これらの結果は無細胞系での実験によって確認された。Deoxyradicinin (**1**) から radicinin (**3**) への変換を触媒する deoxyradicinin 3-monooxygenase は 35 °C、pH 7.0 でもっとも高い活性を示し、その反応に NAD^+ が必要であった。またその分子量は 130–184 kDa と決定された。Radicinin (3)から 3-*epi*-radicinin (**4**)への変換を触媒する radicinin epimerase を酵素抽出物から精製した。Radicinin epimerase は 28 kDa のサブユニットからなるホモダイマーであり、温度 30–35 °C、pH 7.0–9.0 でもっとも高い活性を示すことが明らかとなった。これらの結果から、Fig. 1 に示すような radicinin の生合成および代謝経路の存在が明らかになった。

Fusarium 属菌は有名な土壌病原菌で、多種多様な生理活性二次代謝産物を生産する。*Fusarium* sp. Mj-2 株の培養ろ液抽出物より、既知化合物である anhydrofusarubin (**11**) と、５つの新規な 3-*O*-alkyl-4a,10a-dihydrofusarubin 類

(**12-16**)を単離した。各種機器分析データの解析から、新規化合物の構造を 3-*O*-butyl (**12**)、 3-*O*-3'-methylbutyl (**13**)、 3-*O*-2'-methylbutyl (**14**) 3-*O*-2'-phenylethyl-4a,10a-dihydrofusarubin A (**15**)、および 3-*O*-2'-phenylethyl-4a,10a-dihydrofusarubin A の異性体 (**16**) であると決定した(Fig. 2)。これらの化合物および化合物 12 から調製した 3-*O*-methyl 誘導体(**17**)について抗糸状菌、抗細菌活性の評価を行った。その結果、4a,10a-dihydrofusarubin 類では、C-3 位における *O*-置換基の大きさがその化合物の抗微生物活性に負の影響を与えていることが明らかとなった。

今回の研究により、植物病原糸状菌によって生産される二次代謝産物の発病過程における機能や役割について新たな知見が得られた。

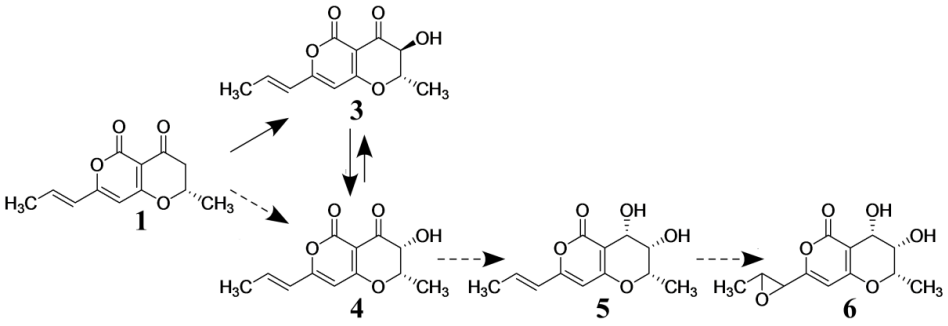

Fig. 1. *Bipolaris coicis* H13-3 株における radicinin (**3**) の生合成，代謝経路

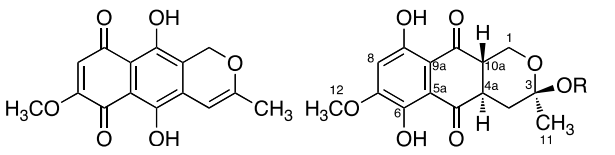

11

12 R=$CH_2CH_2CH_2CH_3$

13 R=$CH_2CH_2CH(CH_3)_2$

14 R=$CH_2CH(CH_3)CH_2CH_3$

15 R=$CH_2CH_2C_6H_5$

17 R=CH_3

Fig. 2. *Fusarium* sp. Mj-2 株から単離された化合物 **11-15** と **17** の化学構造